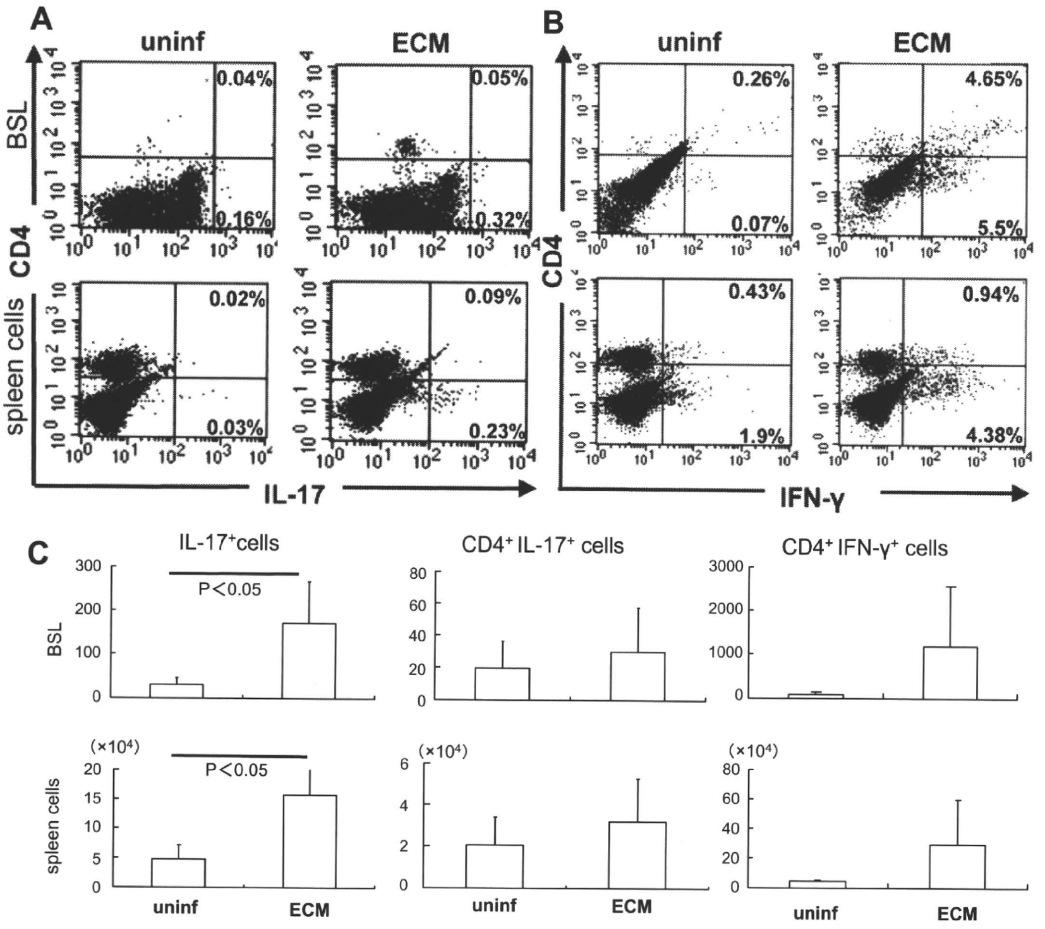

Fig. 2. Induction of IL-17-producing cells during infection with PbA. BSL (upper panel) or spleen cells (lower panel) isolated from mice that developed ECM were analyzed for IL-17 (A) and IFN-γ (B) production. Gated lymphocytes were plotted for CD4 and each cytokine. The numbers indicate the percentage of quadrants. Absolute numbers of the indicated cells were also shown (C). Data represent the mean ± SD of five mice. One representative of at least two repeated experiments is shown.

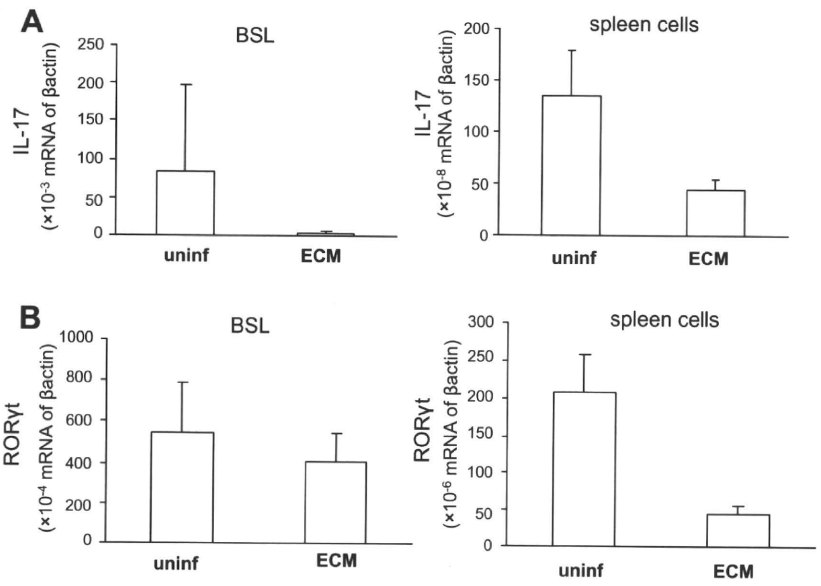

Fig. 3. Induction of Th17 in mice infected with PbA. $CD4^+$ cells were purified from BSL and spleen cells of mice developing ECM and analyzed for the expression of mRNA encoding IL-17 (A) and RORγt (B) as in Fig. 1A. One representative of at least two repeated experiments is shown.

induced by malaria parasites may therefore be independent of IL-23 and IL-17, unlike other infectious diseases.

IL-23 and IL-17 are reported to be protective against some infections [33], yet are responsible for inflammatory pathologies

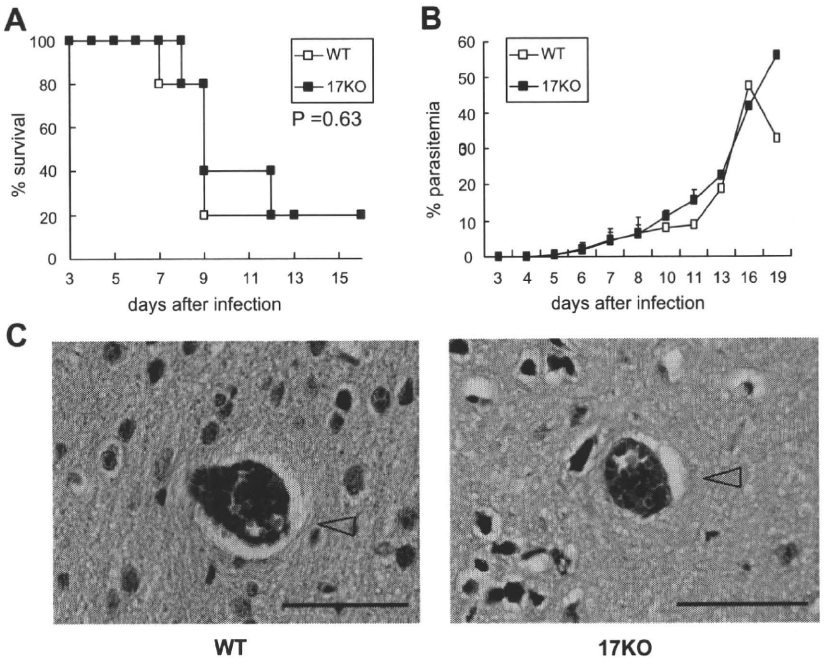

Fig. 4. ECM induced by PbA infection was independent of IL-17. Survival rates (A) or parasitemia (B) of WT and 17KO mice infected with 50,000 PbA-pRBC were monitored as in Fig. 1C. Histological analysis of brain sections of WT (left panels) and 17KO mice (right panels) developing ECM was performed as in Fig. 1E.

in other situations. Parasitemia in P19KO or 17KO mice infected with PbA was similar to that in infected WT mice. These findings suggest that IL-23 and IL-17 do not contribute to the reduction of parasite burdens in mice infected with PbA. However, those cytokines have protective effects against infection with PbNK65 and the lack of IL-23 shortened the survival of infected mice. IL-23 also has anti-protozoan effects against *Plasmodium yoelii* XL (manuscript in preparation). The protective effects of IL-23 and IL-17 during malaria therefore appear to dependent on the species and strain of malaria parasites.

In conclusion, IL-23 and IL-17 are not critical for the development of ECM, a complicated pathology that is produced in association with various immune cells, cytokines and chemokines. It would also be of interest to investigate whether similar results could be achieved using human patients. Such insights will potentially further our understanding CM pathogenesis and help establish new therapeutic strategies.

Acknowledgments

The authors thank Rumiko Koitabashi for handling and support with brain sections. This work was supported by grants from the Ministry of Education, Science Sport and Culture of Japan to H.H. (20390121, 21022036).

Appendix A. Supplementary data

Supplementary data associated with this article can be found, in the online version, at doi:10.1016/j.bbrc.2010.10.114.

References

[1] M.F. Good, H. Xu, M. Wykes, C.R. Engwerda, Development and regulation of cell-mediated immune responses to the blood stages of malaria: implications for vaccine research, Annu. Rev. Immunol. 23 (2005) 69–99.
[2] G.G. MacPherson, M.J. Warrell, N.J. White, S. Looareesuwan, D.A. Warrell, Human cerebral malaria. A quantitative ultrastructural analysis of parasitized erythrocyte sequestration, Am. J. Pathol. 119 (1985) 385–401.
[3] L.H. Miller, D.I. Baruch, K. Marsh, O.K. Doumbo, The pathogenic basis of malaria, Nature 415 (2002) 673–679.
[4] Roll Back Malaria: spotlight on Africa, TDR News (2000) 10, 15.
[5] R.W. Snow, J.F. Trape, K. Marsh, The past, present and future of childhood malaria mortality in Africa, Trends Parasitol. 17 (2001) 593–597.
[6] H.C. van der Heyde, J. Nolan, V. Combes, I. Gramaglia, G.E. Grau, A unified hypothesis for the genesis of cerebral malaria: sequestration, inflammation and hemostasis leading to microcirculatory dysfunction, Trends Parasitol. 22 (2006) 503–508.
[7] R.A. Kastelein, C.A. Hunter, D.J. Cua, Discovery and biology of IL-23 and IL-27: related but functionally distinct regulators of inflammation, Annu. Rev. Immunol. 25 (2007) 221–242.
[8] E. Bettelli, T. Korn, M. Oukka, V.K. Kuchroo, Induction and effector functions of T(H)17 cells, Nature 453 (2008) 1051–1057.
[9] C.L. Langrish, B.S. McKenzie, N.J. Wilson, R. de Waal Malefyt, R.A. Kastelein, D.J. Cua, IL-12 and IL-23: master regulators of innate and adaptive immunity, Immunol. Rev. 202 (2004) 96–105.
[10] W. Sun, X. He, Z. Guo, Q. Wang, X. Li, J. Rayner, L. Zhang, J. Wang, X. Cao, IL-12p40-overexpressing immature dendritic cells induce T cell hyporesponsiveness in vitro but accelerate allograft rejection in vivo: role of NK cell activation and interferon-gamma production, Immunol. Lett. 94 (2004) 191–199.
[11] C.T. Weaver, R.D. Hatton, P.R. Mangan, L.E. Harrington, IL-17 family cytokines and the expanding diversity of effector T cell lineages, Annu. Rev. Immunol. 25 (2007) 821–852.
[12] S.A. Khader, G.K. Bell, J.E. Pearl, J.J. Fountain, J. Rangel-Moreno, G.E. Cilley, F. Shen, S.M. Eaton, S.L. Gaffen, S.L. Swain, R.M. Locksley, L. Haynes, T.D. Randall, A.M. Cooper, IL-23 and IL-17 in the establishment of protective pulmonary $CD4^+$ T cell responses after vaccination and during mycobacterium tuberculosis challenge, Nat. Immunol. 8 (2007) 369–377.
[13] W. Ouyang, J.K. Kolls, Y. Zheng, The biological functions of T helper 17 cell effector cytokines in inflammation, Immunity 28 (2008) 454–467.
[14] E. Bettelli, M. Oukka, V.K. Kuchroo, T(H)-17 cells in the circle of immunity and autoimmunity, Nat. Immunol. 8 (2007) 345–350.
[15] C.M. Tato, D.J. Cua, Reconciling id, ego, and superego within interleukin-23, Immunol. Rev. 226 (2008) 103–111.
[16] J. Knauer, S. Siegemund, U. Muller, S. Al-Robaiy, R.A. Kastelein, G. Alber, R.K. Straubinger, Borrelia burgdorferi potently activates bone marrow-derived conventional dendritic cells for production of IL-23 required for IL-17 release by T cells, FEMS Immunol. Med. Microbiol. 49 (2007) 353–363.
[17] J.S. Stumhofer, A. Laurence, E.H. Wilson, E. Huang, C.M. Tato, L.M. Johnson, A.V. Villarino, Q. Huang, A. Yoshimura, D. Sehy, C.J. Saris, J.J. O'Shea, L. Hennighausen, M. Ernst, C.A. Hunter, Interleukin 27 negatively regulates the development of interleukin 17-producing T helper cells during chronic inflammation of the central nervous system, Nat. Immunol. 7 (2006) 937–945.
[18] D.S. Hansen, N.J. Bernard, C.Q. Nie, L. Schofield, NK cells stimulate recruitment of $CXCR3^+$ T cells to the brain during *Plasmodium berghei*-mediated cerebral malaria, J. Immunol. 178 (2007) 5779–5788.

[19] C. Engwerda, E. Belnoue, A.C. Gruner, L. Renia, Experimental models of cerebral malaria, Curr. Top. Microbiol. Immunol. 297 (2005) 103–143.
[20] L. Chen, Z. Zhang, F. Sendo, Neutrophils play a critical role in the pathogenesis of experimental cerebral malaria, Clin. Exp. Immunol. 120 (2000) 125–133.
[21] S. deWalick, F.H. Amante, K.A. McSweeney, L.M. Randall, A.C. Stanley, A. Haque, R.D. Kuns, K.P. MacDonald, G.R. Hill, C.R. Engwerda, Cutting edge: conventional dendritic cells are the critical APC required for the induction of experimental cerebral malaria, J. Immunol. 178 (2007) 6033–6037.
[22] J. Miu, A.J. Mitchell, M. Muller, S.L. Carter, P.M. Manders, J.A. McQuillan, B.M. Saunders, H.J. Ball, B. Lu, I.L. Campbell, N.H. Hunt, Chemokine gene expression during fatal murine cerebral malaria and protection due to CXCR3 deficiency, J. Immunol. 180 (2008) 1217–1230.
[23] E. Belnoue, M. Kayibanda, A.M. Vigario, J.C. Deschemin, N. van Rooijen, M. Viguier, G. Snounou, L. Renia, On the pathogenic role of brain-sequestered alphabeta $CD8^+$ T cells in experimental cerebral malaria, J. Immunol. 169 (2002) 6369–6375.
[24] T. Voza, A.M. Vigario, E. Belnoue, A.C. Gruner, J.C. Deschemin, M. Kayibanda, F. Delmas, C.J. Janse, B. Franke-Fayard, A.P. Waters, I. Landau, G. Snounou, L. Renia, Species-specific inhibition of cerebral malaria in mice coinfected with *Plasmodium* spp., Infect. Immun. 73 (2005) 4777–4786.
[25] J. Hearn, N. Rayment, D.N. Landon, D.R. Katz, J.B. de Souza, Immunopathology of cerebral malaria: morphological evidence of parasite sequestration in murine brain microvasculature, Infect. Immun. 68 (2000) 5364–5376.
[26] N.H. Hunt, G.E. Grau, Cytokines: accelerators and brakes in the pathogenesis of cerebral malaria, Trends Immunol. 24 (2003) 491–499.
[27] C.L. Maynard, C.T. Weaver, Intestinal effector T cells in health and disease, Immunity 31 (2009) 389–400.
[28] W. O'Connor Jr., M. Kamanaka, C.J. Booth, T. Town, S. Nakae, Y. Iwakura, J.K. Kolls, R.A. Flavell, A protective function for interleukin 17A in T cell-mediated intestinal inflammation, Nat. Immunol. 10 (2009) 603–609.
[29] H. Hisaeda, Y. Maekawa, D. Iwakawa, H. Okada, K. Himeno, K. Kishihara, S. Tsukumo, K. Yasutomo, Escape of malaria parasites from host immunity requires $CD4^+$ $CD25^+$ regulatory T cells, Nat. Med. 10 (2004) 29–30.
[30] T.T. Long, S. Nakazawa, S. Onizuka, M.C. Huaman, H. Kanbara, Influence of $CD4^+$ $CD25^+$ T cells on *Plasmodium berghei* NK65 infection in BALB/c mice, Int. J. Parasitol. 33 (2003) 175–183.
[31] E. Bettelli, Y. Carrier, W. Gao, T. Korn, T.B. Strom, M. Oukka, H.L. Weiner, V.K. Kuchroo, Reciprocal developmental pathways for the generation of pathogenic effector TH17 and regulatory T cells, Nature 441 (2006) 235–238.
[32] A. Bhalla, V. Suri, V. Singh, Malarial hepatopathy, J. Postgrad. Med. 52 (2006) 315–320.
[33] F.L. van de Veerdonk, M.S. Gresnigt, B.J. Kullberg, J.W. van der Meer, L.A. Joosten, M.G. Netea, Th17 responses and host defense against microorganisms: an overview, BMB Rep. 42 (2009) 776–787.

International Immunology Advance Access published February 5, 2010

International Immunology 2010; 1 of 11
doi:10.1093/intimm/dxp126

© The Japanese Society for Immunology. 2010. All rights reserved.
For permissions, please e-mail: journals.permissions@oxfordjournals.org

Transient role of $CD4^+CD25^+$ regulatory T cells in mycobacterial infection in mice

Yuriko Ozeki[1,2], Isamu Sugawara[3], Tadashi Udagawa[3], Toshiaki Aoki[3], Mayuko Osada-Oka[1], Yoshitaka Tateishi[1], Hajime Hisaeda[4], Yuji Nishiuchi[5], Nobuyuki Harada[3], Kazuo Kobayashi[6] and Sohkichi Matsumoto[1]

[1]Department of Bacteriology, Osaka City University Graduate School of Medicine, 1-4-3 Abeno-ku, Osaka 545-8585, Japan
[2]Sonoda Women's University, 7-29-1 Minamitsukaguchi-cho, Amagasaki, Hyogo 661-8520, Japan
[3]Mycobacterial Reference Center, The Research Institute of Tuberculosis, 3-1-24 Matsuyama Kiyose-shi Tokyo, 204-8533, Japan
[4]Department of Microbiology and Immunology, Graduate School of Medical Sciences, Kyushu University, 3-1-1 Maidashi, Higashi-ku, Fukuoka 812-8582, Japan
[5]Peptide Institute Inc., Protein Research Foundation, Minoh-shi, Osaka 562-8686, Japan
[6]Department of Immunology, National Institute of Infectious Diseases, Toyama 1-23-1, Shinjuku-ku, Tokyo 162-8640, Japan

Correspondence to: S. Matsumoto and Y. Ozeki; E-mail. sohkichi@med.osaka-cu.ac.jp and yuriozeki@med.osaka-cu.ac.jp

Transmitting editor: S. Koyasu

Received 22 April 2009, *accepted* 22 December 2009

Abstract

$CD4^+CD25^+$ regulatory T (Treg) cells cause immune suppression by inhibiting T cell effector functions and play pivotal roles not only in self-tolerance but also in immune response to parasitic microbial pathogens. Mycobacteria are major parasitic bacterial pathogens, but the role of $CD4^+CD25^+$ Treg cells in mycobacterial infection is not yet defined. In this study we found that, at the early stage of infection, depletion of $CD25^+$ cells reduced both bacterial load and granuloma formation in mice infected with *Mycobacterium tuberculosis* strains, such as *M. tuberculosis* Erdman or *M. tuberculosis* Kurono. However, at a later stage of infection, bacterial burden and histopathology were similar regardless of depletion of $CD25^+$ cells. Severe combined immunodeficient (SCID) mice reconstituted with $CD4^+CD25^-$ T cells alone or a combination of $CD4^+CD25^+$ and $CD4^+CD25^-$ T cells showed similar bacterial loads and survival kinetics after infection with *M. tuberculosis* Erdman. Consistent with *in vivo* data, *in vitro* studies revealed that mycobacterial antigens, purified protein derivative of tuberculin (PPD), failed to induce the suppressive function of $CD4^+CD25^+$ Treg cells to $CD4^+CD25^-$ effector T cells, as demonstrated by the lack of response of $CD4^+CD25^+$ T cells to PPD, in mice chronically infected with *Mycobacterium bovis* bacillus Calmette–Guérin and *M. tuberculosis*. Our data show that $CD4^+CD25^+$ Treg cells have a transient effect at the early stage of mycobacterial infection but, contrary to the expectation, have little impact on the overall course of infection.

Keywords: bacterial, T cells, rodent, inflammation, lung

Introduction

Mycobacteria are intracellular bacterial pathogens, which persistently infect eukaryotes, including mammals, and cause diseases not only following primary infection but also by reactivation from latent state. Several species of mycobacteria, such as *Mycobacterium tuberculosis* and *Mycobacterium bovis*, are known to cause human tuberculosis. The World Health Organization estimates that *M. tuberculosis* infects one-third of the world's population and is responsible for 2 million deaths each year (1). While the infection remains latent in 95% of the infected cases of *M. tuberculosis*, 5–10% of those who initially controlled the infection later develop active disease at some stage during their lifetime. To suppress intracellular growth of mycobacteria, macrophage activation by IFN-gamma is critical in both mice (2, 3) and humans (2, 3).

The important role of the $CD4^+CD25^+$ regulatory T (Treg) cells in immune response has recently been recognized. This T cell subset maintains immunologic self-tolerance and suppresses the onset of autoimmune diseases (4). The vast majority of Treg cells constitutively express CD25/IL-2 receptor alpha chain in the physiological state (5, 6). $CD4^+CD25^+$ Treg cells also express cytotoxic T-lymphocyte-associated protein 4 (CTLA-4; 7, 8), glucocorticoid-induced tumor necrosis factor receptor (GITR; 9, 10) and the transcription factor,

FoxP3 (11, 12). Some subsets of $CD4^+CD25^+$ Treg cells also produce effector cytokines, such as IL-10 and transforming growth factor (TGF)-β (13, 14). The defining feature of $CD4^+CD25^+$ Treg cells is their ability to inhibit the proliferation of T cells and IFN-gamma production through cell–cell contact (15, 16), possibly mediated by CTLA-4, and/or through the production of immunosuppressive cytokines, such as TGF-β and IL-10 (13, 14).

Recently, it has been reported that $CD4^+CD25^+$ Treg cells are also involved in suppressive immune responses during several infectious diseases. Depletion of $CD4^+CD25^+$ Treg cells enhances anti-microbial activity against diverse pathogens including the protozoan *Leishmania major* and *Plasmodium yoelii*, viruses such as HIV and Herpes simplex virus and bacteria such as *Helicobacter pylori* (17–21).

In spite of suggested importance of $CD4^+CD25^+$ Treg cells in parasitic pathogens, the knowledge in mycobacterial infection remains controversial (22–25). Kursar *et al.* and Scott-Browne *et al.* showed that Treg cells prevented protective immunity against *M. tuberculosis* infection by utilizing reconstituted and chimeric mice, respectively (22, 25). In contrast, Quinn *et al.* suggested minor role of $CD4^+CD25^+$ in both *Mycobacterium bovis* bacillus Calmette Guérin (BCG)-induced protection and natural mycobacterial infection (23, 24). In order to elucidate the roles of $CD4^+CD25^+$ Treg cells in mycobacterial infection more precisely, we carried out the experiments using Treg-deleted mice by antibody to CD25 molecule and SCID mice reconstituted with T cell subsets. We found that mycobacterial antigen-specific $CD4^+CD25^+$ Treg cells were hardly developed after mycobacterial infection in mice and therefore the function of $CD4^+CD25^+$ Treg cells was limited after the infection was established. Thus, $CD4^+CD25^+$ Treg cells have little impact on the overall course of mycobacterial infection.

Methods

Mice

Specific pathogen-free, female DBA/2 mice aged 6 weeks were purchased from Japan SLC (Shizuoka, Japan). BALB/c and SCID/BALB/c mice were purchased from Japan CLEA (Tokyo, Japan). All mice were maintained under specific pathogen-free conditions in the animal facilities of Osaka City University Graduate School of Medicine and in a biosafety-level-3 facility at The Research Institute of Tuberculosis according to the standard guidelines for animal experiments at each institute with approval of their ethical committees.

Depletion of $CD4^+CD25^+$ cells

A hybridoma cell line expressing anti-mouse CD25 monoclonal IgM [a monoclonal antibody against mouse CD25 (7D4), American Type Culture Collection, Manassas, VA, USA] was expanded as ascites in pristine-primed SCID mice (Wako, Osaka, Japan). The Ig-rich fraction was obtained by 30% ammonium sulfate precipitation of ascitic fluid followed by dialysis in PBS. An isotype-matched control IgM was purchased from eBioscience (San Diego, CA, USA). The protein concentration was determined by Bradford's method using BSA (Sigma–Aldrich, St Louis, MO, USA) as a standard. For depletion of $CD25^+$ cells in early stage of infection, mice were injected with 1 mg of 7D4 or control IgM intraperitoneally (i.p.) 1 day before, and then 3 and 10 days after *M. tuberculosis* infection. For depletion of $CD25^+$ cells in late stage of infection, mice were injected (i.p.) with 1 mg of 7D4 or control IgM at 60, 65 and 70 days after *M. tuberculosis* infection. Depletion of $CD4^+CD25^+$ cells was assessed by flow cytometry using a FACScan (Becton Dickinson, Franklin Lakes, NJ, USA). Peripheral blood leukocytes (PBLs) were obtained by incubation with 0.83% ammonium chloride solution at 37°C for 5 min to induce erythrocyte lysis. PBLs or splenocytes were stained with PE-conjugated anti-CD4 mAb (GK1.5, eBioscience) and FITC-conjugated anti-CD25 mAb (PC61, eBioscience). The data were analyzed by flow cytometry with using Cellquest™ software (Becton Dickinson).

Bacteria and infection

Mycobacterium bovis BCG Tokyo, *M. tuberculosis* H37Rv, *M. tuberculosis* Kurono (ATCC 35812) and *M. tuberculosis* Erdman were grown in 7H9 medium (Difco, Detroit, MI, USA) supplemented with 10% BSA, dextrose and catalase enrichment (Difco) and 0.05% Tween 80 at 37°C to mid-logarithmic phase, then stored in frozen aliquots as previously described (26). For infection with *M. tuberculosis* Kurono and *M. tuberculosis* Erdman, the nebulizer of a Middlebrook airborne infection apparatus (Glas-col, Terre Haute, IN, USA) was filled with 5 ml PBS containing 5×10^6 colony-forming units (CFU) of bacteria and the mice were airborne infected for 90 min by Glas-Col aerosol generator. This procedure deposits ~10 CFU of bacteria into the lungs. At 0, 3 and 5 weeks (and also 2 weeks in some experiments) post-infection, three to five mice per group were euthanized and the lungs, livers and spleens were harvested. The organs were homogenized in 1 ml sterile distilled water using a mortar and pestle and serial dilutions were plated onto Middlebrook 7H11 agar containing oleic acid, dextrose, albumin and catalase enrichment (Difco) (7H11-OADC agar). Bacterial numbers were counted using CFU after culturing at 37°C for 20–30 days. To investigate the role of $CD4^+CD25^+$ Treg cells in the late stage of infection, mice were airborne-infected with *M. tuberculosis* H37Rv as the same method described above and $CD25^+$ cells were depleted by 7D4 treatment on days 60, 65, and 70. At 75 days post-infection, eight mice per group were euthanized and bacterial numbers in lungs and spleens were determined by CFU count and histological evaluation were performed as the same procedures described above.

Isolation of $CD4^+CD25^+$ T cells and $CD4^+CD25^-$ T cells

BALB/c mice were infected i.p. with 5×10^4 CFU of *M. bovis* BCG Tokyo. $CD4^+CD25^+$ T cells and $CD4^+CD25^-$ T cells were purified from spleens of normal mice or chronically BCG-infected (>6 months post-infection) BALB/c mice using $CD4^+CD25^+$ regulatory T cell isolation kit (Miltenyl Biotec, Bergisch Gladgach, Germany) after depleting erythrocytes with 0.83% ammonium chloride solution. Obtained cells were labeled with PE-conjugated anti-CD25 mAb, stained with FITC-conjugated anti-CD4 mAb (eBioscience) and analyzed

by flow cytometer. The purity of selected populations was confirmed as >96%. Expression of foxp3 in the $CD4^+CD25^+$ T cell population was confirmed using flow cytometer after intracellular staining with anti-FITC-conjugated anti-mouse foxp3 mAb (eBioscience). $CD4^+CD25^+$ T cells stained by this procedure were >90% foxp3-positive. Non-$CD4^+$ cells of normal mice retained in the MACS separation column were flushed out and incubated for >2 h. Attached cells were used as antigen-presenting cells (APCs) after treatment with 20-Gy radiation. T cell populations and APCs were also isolated from DBA/2 mice chronically infected with *M. tuberculosis* as the similar procedure with BCG-infected mice described above. However, in this case, to obtain APCs, spleen cells of normal DBA/2 mice were incubated for >2 h and attached cells were treated with mitomycin C (50 μg zml^{-1}) for 30 min at 37°C instead of radiation.

In vitro T cell proliferation assay and measurement of cytokines

$CD4^+CD25^+$ T cells and $CD4^+CD25^-$ T cells were prepared to be 1×10^6 cells ml^{-1}. Various ratios of $CD4^+CD25^+$ T cells and $CD4^+CD25^-$ T cells were cultured for 5 or 7 days with 10 μg ml^{-1} of purified protein derivative of tuberculin (PPD) or anti-CD3 mAb (CEDARLANE, Canada) in the presence of 1×10^5 cells ml^{-1} of APC in 96-well plates in RPMI 1640 supplemented with 10% FCS, 2 mM L-glutamine, penicillin (100 U ml^{-1}), streptomycin (100 mg ml^{-1}) and 50 mM 2-mercaptoethanol. Proliferation was evaluated by pulsing cells with 1 μCi (37 kBq) per well [^{3}H]thymidine ([^{3}H]TdR) for 6 h and [^{3}H]TdR incorporation measured using a scintillation counter. In the experiments to analyze the function of T cells derived from *M. tuberculosis*-infected mice, proliferation was evaluated by incorporation of 5-bromo-2′-deoxyuridine (BrdU) using a commercially available kit (Cell proliferation ELISA, BrdU colorimetoric, Roche, Germany). Production of IFN-gamma, IL-10, IL-2 and IL-6 in the culture supernatant was measured using a commercially available ELISA kit (R&D System, Minneapolis, MN, USA).

Transfer of T cell population into SCID mice

$CD4^+CD25^+$ T cells and $CD4^+CD25^-$ T cells were purified from the spleens of BALB/c mice chronically infected with BCG using $CD4^+CD25^+$ Treg cell isolation kit. Totally, 7.5×10^5 $CD4^+CD25^-$ T cells or 7.5×10^5 $CD4^+CD25^+$ T cells either alone or in combination (7.5×10^5 $CD4^+CD25^-$ T cells and 7.5×10^4 $CD4^+CD25^+$ T cells) were transferred intravenously to cognate SCID mice (17). One day after transfer, recipient mice were infected aerogenically with *M. tuberculosis* Erdman as described above. Three weeks post-infection, five to eight mice were euthanized and bacterial burden was counted. The survival time course of seven mice per group was observed for up to 165 days post-infection.

Neutralization of IL-6 in culture supernatant

$CD4^+CD25^-$ T cells, $CD4^+CD25^+$ T cells and APCs were isolated from chronically BCG-infected mice according to the procedures described above. Anti-mouse IL-6-neutralizing mAb (Biolegend, San Diego, CA, USA) or isotype-matched control antibody (Southern Biotech, Birmingham, AL, USA) was added to the culture of $CD4^+CD25^-$ effector T cells either alone or in combination with $CD4^+CD25^+$ T cells at concentration of 0.02 μg ml^{-1} and cultured for 4 days in the presence of PPD or anti-CD3 mAb. IFN-gamma production and [^{3}H]TdR incorporation were measured after 4 days incubation.

Transfer of culture medium

T cell subsets were obtained from chronically BCG-infected mice as described above. $CD4^+CD25^-$ T cells/$CD4^+CD25^+$ T cells/APCs (1:0:0.1) or $CD4^+CD25^-$ T cells/$CD4^+CD25^+$ T cells/APCs (1:1:0.1) were cultured with PPD or anti-CD3 mAb for 7 days and each culture supernatant stored at −80°C until later use. Freshly isolated $CD4^+CD25^-$ T cells/$CD4^+CD25^+$ cells/APCs (1:0:0.1) or $CD4^+CD25^-$ T cells/$CD4^+CD25^+$ T cells/APCs (1:1:0.1) were cultured with stored supernatant:new medium (1:1) in the presence or absence of anti-CD3 mAb. On day 4, [^{3}H]TdR incorporation was measured as described above.

In vitro activation of $CD4^+CD25^+$ T cells

$CD4^+CD25^+$ T cells isolated from chronically infected BALB/c mice with BCG or *M. tuberculosis* H37Rv were incubated with Dynabeads Mouse CD3/CD28 T cell Expander (Invitrogen, Norway) at a bead:cell ratio of 2:1 adding 2000 U ml^{-1} of recombinant mouse IL-2 according to the manufacturer's protocol. Two days after incubation, the beads were

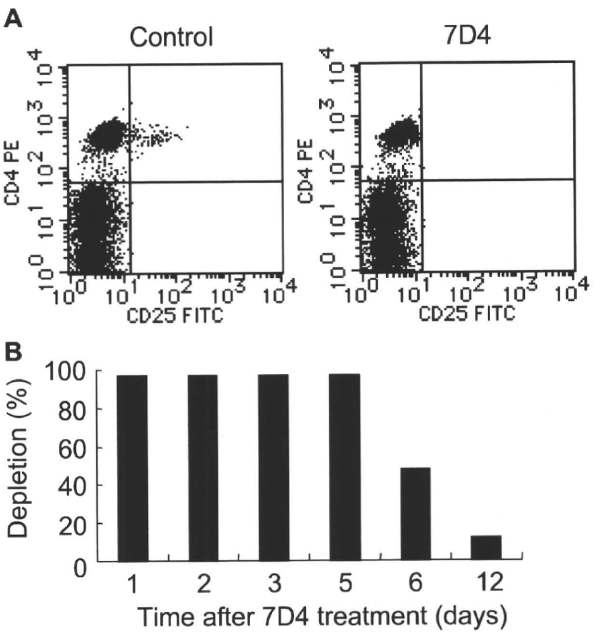

Fig. 1. Selective loss of $CD4^+CD25^+$ T cells by treatment with anti-CD25 mAb, 7D4. (A) Flow cytometric analysis of PBLs obtained from i.p.-injected mice with 1 mg of anti-CD25 mAb (7D4) or control IgM (control) 1 day after injection. Cells were stained with FITC-conjugated anti-CD25 mAb (PC61) and PE-conjugated anti-CD4 mAb (GK1.5). (B) Time course of the level of depletion of $CD4^+CD25^+$ T cell in PBL after a single dose of 7D4. Data are expressed as percent depleted relative to the $CD4^+CD25^+$ cell population in control IgM-treated mice. Data are mean of three mice per time point.

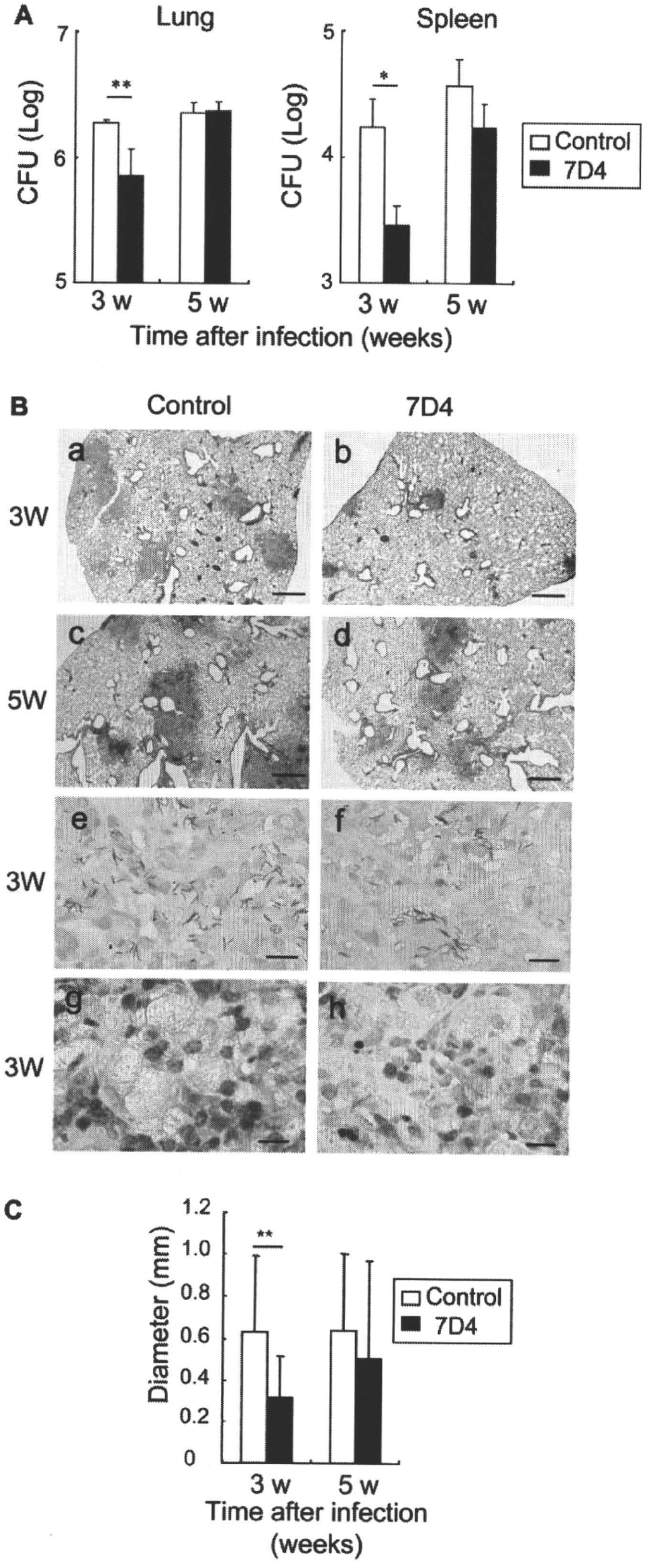

Fig. 2. The effect of $CD25^+$ cell depletion in *Mycobacterium tuberculosis* Kurono infection in mice. DBA/2 mice treated with 1 mg of 7D4, anti-CD25 mAb or control IgM were aerogenically infected with 5×10^6 CFU of *M. tuberculosis* Kurono. (A) Bacterial numbers were counted in lungs (left panel) and spleens (right panel) of mice treated with control IgM (open bars) or with 7D4, anti-CD25 mAb (closed bars). (B) Histopathological features of lungs from *M. tuberculosis* Kurono-infected mice. Lung sections were stained with H&E (a–d), Ziehl–Neelsen (e and f) and Giemsa (g and h). Granulomas mainly consisted of epithelioid macrophages (g and h). Numerous acid-fast bacteria were observed in granulomas of both control IgM-treated and anti-CD25 mAb-treated (7D4) mice. (a, c, e and g) Lungs sections from mice treated with control IgM. (b, d, f and h) Lungs sections from mice treated with 7D4. (a, b and e–h) Three weeks after infection. (c and d) Five weeks after infection. Bars, 500 μm (a–d), 10 μm (e-h). (C) The diameter of granulomatous lesions was measured in the lung sections from mice treated with control IgM (open bars) or with 7D4, anti-CD25 mAb (closed bars). Bars represent mean ±standard deviation of three to five mice. $*P < 0.05$ versus control mice; $**P < 0.01$ versus control mice.

removed from $CD4^+CD25^+$ T cells by magnet. After washing with medium, cells were used as activated $CD4^+CD25^+$ T cells. Freshly isolated $CD4^+CD25^-$ effector T cells were incubated with activated $CD4^+CD25^+$ T cells in the presence of PPD.

Histological analysis

Tissues were removed from mice at various intervals, fixed in 10% formalin and embedded in paraffin blocks. Sections (5 μm) were stained with hematoxylin and eosin (H&E), Ziehl–Neelsen or Giemsa methods. To evaluate the intensity of inflammatory response of the lung, the mean diameters of pulmonary granulomas were measured in three sections per mouse using Microanalyzer (Poladigital, Tokyo, Japan).

Statistical analysis

Results were analyzed by one-way analysis of variance (ANOVA) by SAS system R.8.1. Data were expressed as mean values ± standard deviation and considered significant if $P < 0.05$.

Results

Depletion of $CD25^+$ cells in early stage of infection causes transient effect on in vivo growth of M. tuberculosis Kurono and M. tuberculosis Erdman

7D4 is a mAb against mouse CD25. Administration of 1 mg 7D4 into a mouse resulted in the loss of >96% of $CD4^+CD25^+$ T cells in the peripheral blood and spleens (Fig. 1A). Loss of $CD25^+$ cells maintained at least for 5 days after 7D4 treatment (Fig. 1B). Depletion of $CD25^+$ cells by 7D4 protects mice from death caused by infection of *Plasmodium yoelii*, suggesting a role for $CD4^+CD25^+$ Treg cells in exacerbating malaria (21).

Using 7D4, we first depleted $CD25^+$ cells of DBA/2 mice and then infected animals with 5×10^6 CFU/mouse of *M. tuberculosis* Kurono, which was clinically isolated strain in Japan, by airborne infection. Bacterial load in lung and spleen, and histopathology of the lung were monitored at 3 and 5 weeks post-infection. *Mycobacterium tuberculosis* Kurono multiplied to approximately 2×10^6 CFU per lung 3 weeks post-challenge and maintained these bacterial numbers 5 weeks post-challenge. In spleens, we detected 2×10^4 and 3×10^4 CFU per organ 3 and 5 weeks

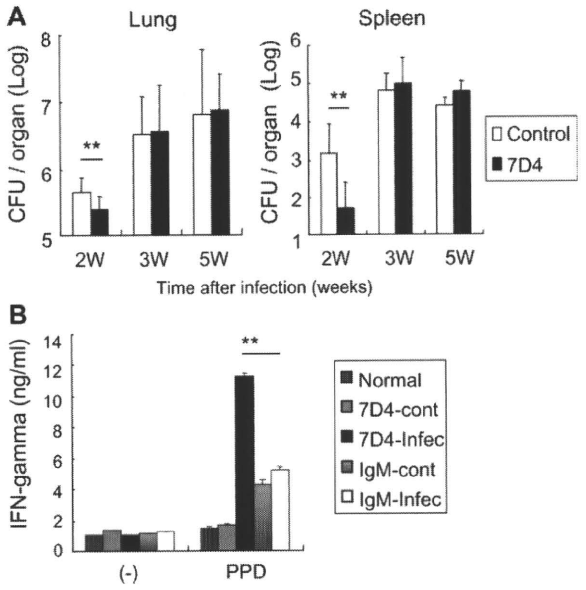

Fig. 3. The effect of CD25$^+$ cell depletion in *Mycobacterium tuberculosis* Erdman infection. (A) Control IgM-treated mice (open bars) and 7D4 anti-CD25 antibody-treated-mice (closed bars) were aerogenically infected with 5×10^6 CFU of *M. tuberculosis* Erdman. Bacterial numbers of lungs and spleens were measured at 2, 3 and 5 weeks post-infection. $^{**}P < 0.01$ versus control mice. (B) CD4$^+$ T cells from non-infected mice with 7D4 treatment (7D4-cont), *M. tuberculosis*-infected mice with 7D4 treatment (7D4-Infec), non-infected mice with control IgM treatment (IgM-cont) or *M. tuberculosis*-infected mice with control IgM treatment (IgM-Infec) were cultured with APC in the presence (PPD) or absence (−) of 10 μg ml^{-1} PPD for 7 days. Production of IFN-gamma in the culture supernatants was analyzed. $^{**}P < 0.01$: *Mycobacterium tuberculosis*-infected mice with control IgM treatment (IgM-Infec) versus *M. tuberculosis*-infected mice with 7D4 treatment (7D4-Infec).

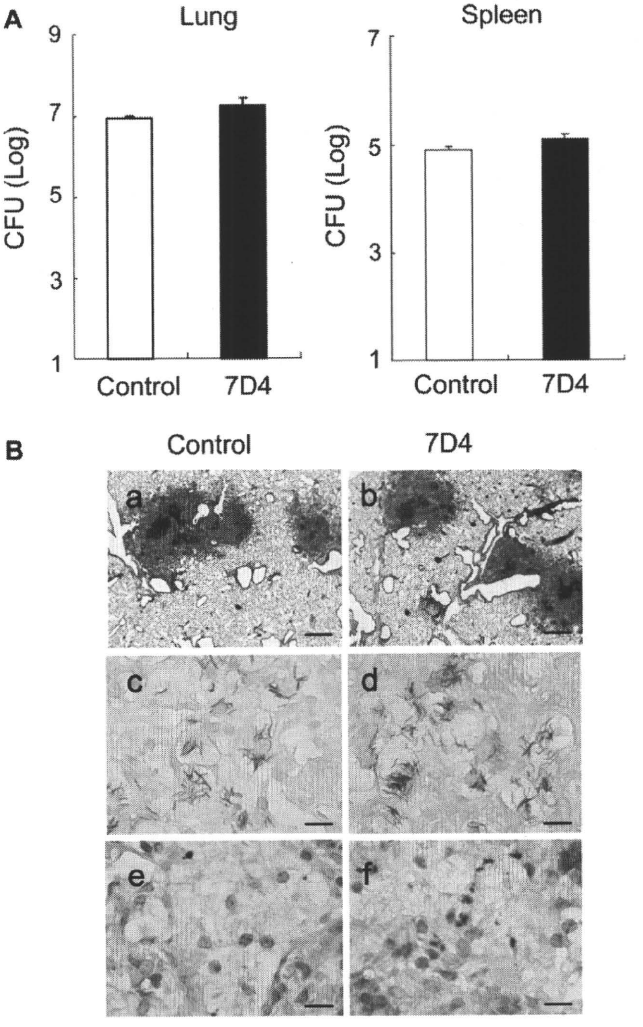

Fig. 4. The effect of depletion of CD25$^+$ cell in chronically infected mice with *M. tuberculosis*. DBA/2 mice were aerogenically infected with 5×10^6 CFU of *M. tuberculosis* H37Rv. Two months after infection, mice were treated with 1 mg of 7D4 or control IgM three times with 4 days interval. Five days later from final treatment, mice were sacrificed and analyzed. (A) Bacterial numbers in lungs (left panel) and spleens (right panel) of mice treated with control IgM (open bars) or 7D4 (closed bars). (B) Lung sections were stained with H&E (a and b), Ziehl–Neelsen (c and d) and Giemsa (e and f). Granulomas mainly consisted epithelioid macrophages (e and f). Numerous acid-fast bacteria were observed in granulomas of both control IgM- and 7D4-treated mice. (a, c and e) Lungs sections from mice treated with control IgM. (b, d and f) Lungs sections from mice treated with 7D4. Bars, 500 μm (a and b), 10 μm (c–f). Bars represent mean ±standard deviation of eight mice.

post-challenge, respectively (Fig. 2A). Depletion of CD25$^+$ cells resulted in significantly lower bacterial number in both lung and spleen 3 weeks after challenge; however, this effect became marginal 5 weeks post-challenge (Fig. 2A). Numerous bacteria were observed in granulomas of 7D4-treated and control mice after infection (Fig. 2B, e and f), consistent with higher bacterial burdens revealed by plating of organ homogenates (Fig. 2A). Histological examination of the lung correlated with the CFU results; 3 weeks post-infection, depletion of CD25$^+$ cells resulted in decreased granuloma formation compared with mice treated with control IgM, but normalized 5 weeks after challenge [Fig. 2B(a–d) and C]. Histopathology showed that granuloma cellular composition did not differ between 7D4-treated mice and control mice, which consisted predominately of epithelioid macrophages (Fig. 2B, g and h). Thus in *M. tuberculosis* Kurono infection, the effect of CD25$^+$ cell depletion was limited to the early phase of infection only.

To determine whether the transient effect of CD25$^+$ cells is specific for *M. tuberculosis* Kurono, we performed similar experiments employing another commonly used mycobacterial strain, *M. tuberculosis* Erdman. Similar results were observed in bacterial burdens: 7D4-treated mice revealed significantly lower bacterial numbers than those of IgM-treated mice at early stage (2 weeks post-infection), but not 3 weeks or 5 weeks post-challenge (Fig. 3A). Splenic CD4$^+$ T cells derived from 7D4-treated mice at this time point produced significantly higher levels of IFN-gamma than those of IgM-treated mice when stimulated with PPD (Fig. 3B).

We also examined the effects of depletion of CD25$^+$ cells on the survival of another mycobacterial strain, *Mycobacterium bovis* bacillus Calmette-Guérin (BCG). DBA/2 or BALB/c mice depleted of CD25$^+$ cells by 7D4 were challenged with BCG intravenously and the survival of BCG in the lungs

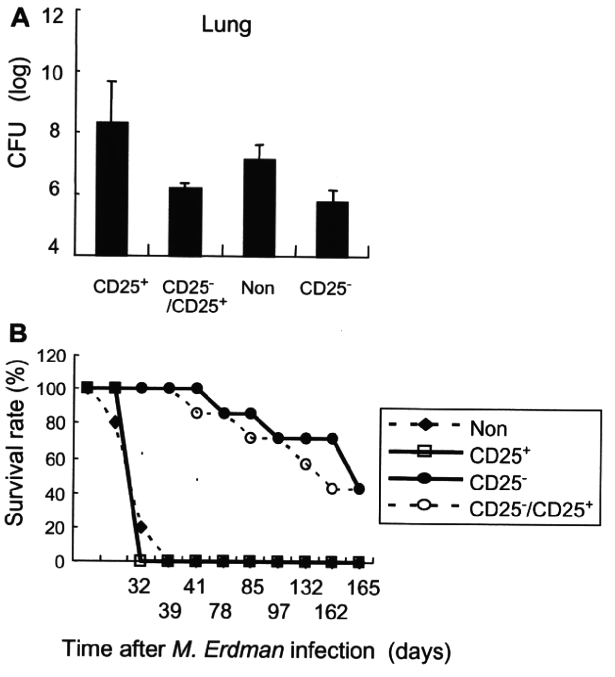

Fig. 5. Bacterial burden and survival kinetics of reconstituted SCID mice with T cell subsets after infection of *Mycobacterium tuberculosis* Erdman. (A) T cell subsets were isolated from spleens of chronically BCG-infected mice. SCID mice were reconstituted with 7.5×10^5 of $CD4^+CD25^+$ T cells only ($CD25^+$), 7.5×10^5 of $CD4^+CD25^-$ T cells and 7.5×10^4 of $CD4^+CD25^+$ T cells ($CD25^-/CD25^+$), untransferred (Non), and 7.5×10^5 of $CD4^+CD25^-$ T cells only ($CD25^-$). One day after reconstitution, naive or T cell subset-reconstituted SCID mice were aerogenically infected with 5×10^6 CFU *M. tuberculosis* Erdman. (B) Survival rates of naive or reconstituted SCID mice after infection. Time course of survival was examined up to 165 days post-infection. Five to eight mice per group were analyzed.

post-challenge was monitored. Unlike *M. tuberculosis*, there was no marked increase in BCG levels in the mouse lungs. Depletion of $CD25^+$ cells did not alter the survival ratio of BCG in the lungs of DBA/2 and BALB/c mice 3 and 5 weeks post-infection, although *in vitro* stimulation with PPD, lymphocytes derived from 7D4-treated mice at 3 weeks after challenge produced higher amount of IFN-gamma than those from control IgM-treated mice (data not shown).

Depletion of $CD25^+$ cells in the chronic stage of infection does not affect the bacterial burdens and pathology

We next examined the effects of depletion of $CD25^+$ cells in the late stage of mycobacterial infection. DBA/2 mice were airborne-infected with *M. tuberculosis* H37Rv and $CD25^+$ cells were depleted by 7D4 treatment after 60, 65 and 70 days later. Five days later from the final treatment of 7D4, we analyzed the bacterial burden and histology in the organs. Bacterial numbers of lungs and spleens in 7D4-treated mice were rather slightly higher than those in control IgM-treated mice; however, significant differences were not observed (Fig. 4A). Pulmonary granuloma formation was conspicuous in both 7D4-treated mice and control IgM-treated mice (Fig. 4B, a and b). Cellular composition of granuloma did not differ between 7D4-treated mice and control mice and numerous bacteria were observed in both groups of mice (Fig. 4B, c–f).

$CD4^+CD25^+$ T cells do not suppress protection induced by $CD4^+CD25^-$ T cells against M. tuberculosis infection in reconstituted mice

To further evaluate the role of $CD4^+CD25^+$ Treg cells in mycobacterial infection at late stage (after developing acquired immunity), the following experiment was conducted. $CD4^+CD25^-$ T cells and $CD4^+CD25^+$ T cells were purified from chronically BCG-infected mice: >90% of the $CD4^+CD25^+$ T cells obtained expressed FoxP3 as estimated by FACScan (data not shown). Each T cell subset, either alone or in combination, was then transferred into SCID mice and mice were infected with *M. tuberculosis* Erdman by airborne exposure. Three weeks post-infection, the bacterial number in lungs (Fig. 5A) and survival kinetics of mice (Fig. 5B) were analyzed.

Observed increases in *M. tuberculosis* were similar in both naive SCID mice and SCID mice reconstituted with $CD4^+CD25^+$ T cells alone, suggesting that $CD4^+CD25^+$ T cells offer no protection against *M. tuberculosis*. In contrast, SCID mice reconstituted with $CD4^+CD25^-$ T cells controlled *M. tuberculosis* infection, at a similar level to that of mice reconstituted with the combination of $CD4^+CD25^-$ T cells and $CD4^+CD25^+$ T cells (Fig. 5A). The survival kinetics showed similar outcomes between mice reconstituted with $CD4^+CD25^-$ T cells plus $CD4^+CD25^+$ T cells and $CD4^+CD25^-$ effector T cells alone (Fig. 5B). These data suggest that the role of $CD4^+CD25^+$ Treg cells in host protection is marginal against *M. tuberculosis* in the overall course of infection (Fig. 5B).

Stimulation with mycobacterial antigens fails to express the function of $CD4^+CD25^+$ Treg cells in vitro

To ascertain why $CD4^+CD25^+$ Treg cells have only a minor role in the late stage of mycobacterial infection, we compared the action of $CD4^+CD25^+$ T cells to $CD4^+CD25^-$ T cells *in vitro*. $CD4^+CD25^+$ and $CD4^+CD25^-$ T cells were isolated from normal mice or mice chronically infected with BCG or *M. tuberculosis* and stimulated with PPD or anti-CD3 mAb in the presence of APCs. $CD4^+CD25^+$ T cells alone showed characteristics of Treg cells, which neither proliferate nor produce cytokines in response to neither PPD nor anti-CD3 mAb (Fig. 6, A–J and a–e). Culture experiments using a combination of $CD4^+CD25^+$ and $CD4^+CD25^-$ T cells showed that $CD4^+CD25^+$ T cells derived from both normal and infected mice suppressed proliferation of $CD4^+CD25^-$ T cells and production of cytokines, such as IFN-gamma and IL-10, in a dose-dependent manner following stimulation with anti-CD3 mAb, showing the characteristics in Treg cells. However, following stimulation with PPD, $CD4^+CD25^+$ T cells failed to suppress both proliferation and production of cytokines. In contrast, IL-2 production was suppressed in a dose-dependent manner in the presence of PPD. Definitive IL-6 production was observed when $CD4^+CD25^-$ T cells were incubated alone or combination with $CD4^+CD25^+$ T cells in the presence of PPD (Fig. 6, I, J and e).

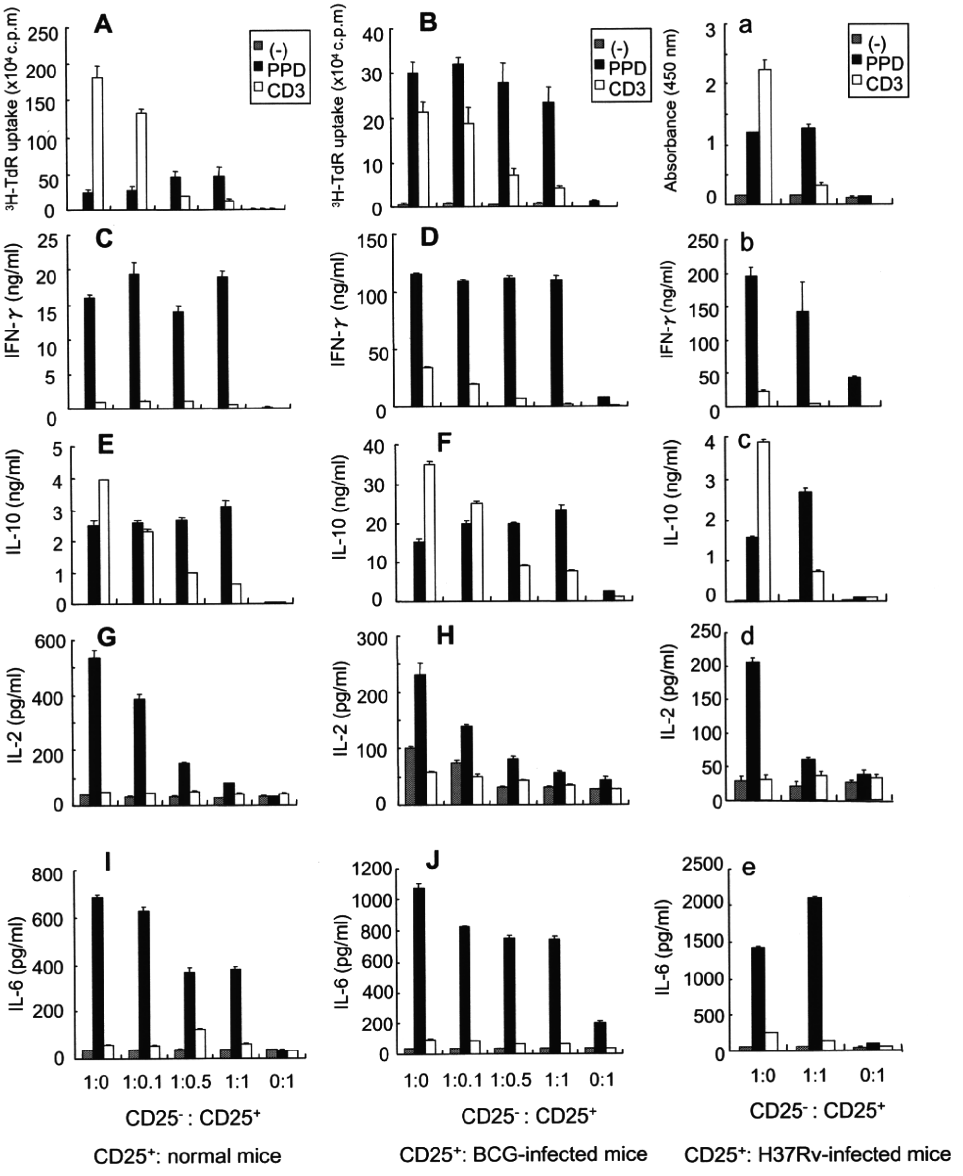

Fig. 6. Stimulation of CD4$^+$CD25$^+$ T cells by PPD fails to suppress the function of PPD-activated CD4$^+$CD25$^-$ T cells. CD4$^+$CD25$^+$ T cells (CD25$^+$) purified from normal (A, C, E, G and I) mice or mice chronically infected with BCG (B, D, F, H and J) or *Mycobacterium tuberculosis* (a–e) were co-cultured with CD4$^+$CD25$^-$ effector T cells (CD25$^-$) purified from mice chronically infected with BCG or *M. tuberculosis* at various ratios with T cell-depleted irradiated spleen cells (APCs) in the presence of PPD (PPD), or anti-CD3 mAb (CD3), or alone (–). Proliferative responses were analyzed at day 5 (A, B and a). Cytokine production in culture supernatants was measured at day 7 (C, E, I, J and b–e) or day 5 (D, F, G and H).

Soluble mediators are not suppressive factors of CD4$^+$CD25$^+$ Treg cell function when stimulated with PPD

Because IL-6 allows effector T cells to overcome suppression by CD4$^+$CD25$^+$ Treg cells (27), we considered the possibility that IL-6 inhibits the function of CD4$^+$CD25$^+$ Treg cells when stimulated with *M. tuberculosis*-derived mycobacterial antigen, PPD. Therefore, we neutralized IL-6 by neutralizing mAb; however, neutralization of IL-6 did not recover suppressive activity of CD4$^+$CD25$^+$ Treg cells (Fig. 7A and B).

To determine whether soluble factors beside IL-6 abrogate the suppressive function of CD4$^+$CD25$^+$ Treg cells upon PPD stimulation, we examined the effects of soluble factors released from T cells and APCs. The culture supernatants from CD4$^+$CD25$^+$ T cells cultured with both CD4$^+$CD25$^-$ T cells and APCs in the presence of PPD or anti-CD3 mAb were collected and then transferred to fresh culture of CD4$^+$CD25$^-$ T cells, CD4$^+$CD25$^+$ T cells and APCs in the presence or absence of anti-CD3 mAb. The proliferative response of CD4$^+$CD25$^-$ effector T cells was analyzed by incorporation of [^{3}H]TdR. The results showed that the supernatants of combined CD4$^+$CD25$^-$ and CD4$^+$CD25$^+$ T cell culture failed to diminish suppressive activity of proliferative response of CD4$^+$CD25$^-$ T cells by CD4$^+$CD25$^+$ T cell stimulated with anti-CD3 mAb (Fig. 8). These results show

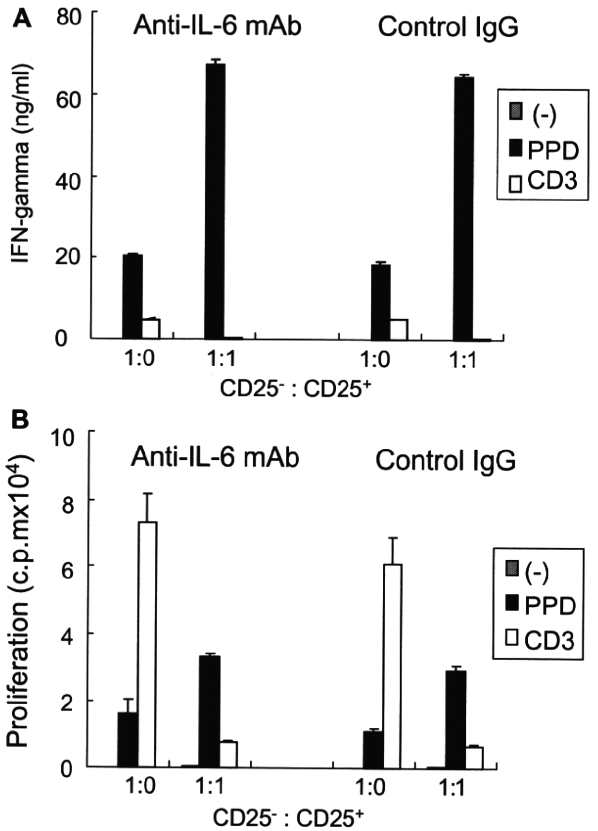

Fig. 7. Neutralization of IL-6 does not affect the $CD4^+CD25^+$ T cell-mediated suppression of the function of effector T cells. $CD4^+CD25^-$ T cells and $CD4^+CD25^+$ T cells were isolated from mice chronically infected with BCG. $CD4^+CD25^-$ effector T cells alone (1:0) or combination of $CD4^+CD25^-$ effector T cells and $CD4^+CD25^+$ T cells (1:1) were cultured with APCs in the presence of PPD (PPD), anti-CD3 mAb (CD3) or absence of these (–). In each well, 0.02 μg ml^{-1} of anti-IL-6 mAb or control IgG were added. IFN-gamma production in culture supernatant (A) and proliferative responses of T cells (B) were analyzed at day 4.

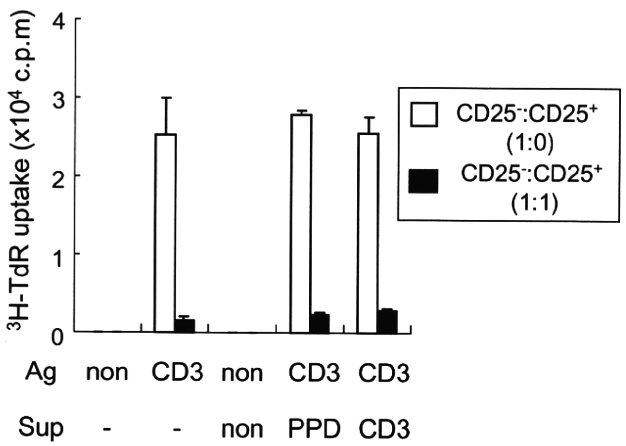

Fig. 8. Soluble mediators upon PPD stimulation do not abrogate $CD4^+CD25^+$ T cell-mediated suppression. $CD4^+CD25^-$ effector T cells ($CD25^-$) and $CD4^+CD25^+$ T cells ($CD25^+$) were isolated from spleens of chronically BCG-infected mice. $CD4^+CD25^-$ T cells/$CD4^+CD25^+$ T cells/APC (1:0:0.1) or $CD4^+CD25^-$ T cells/$CD4^+CD25^+$ cells/APC (1:1:0.1) were cultured with PPD (Sup, PPD), anti-CD3 mAb (Sup, CD3) or alone (Sup, non), for 7 days. Each culture supernatant was stored. Freshly isolated $CD4^+CD25^-$ T cells/$CD4^+CD25^+$ cells/APC (1:0:0.1) or $CD4^+CD25^-$ T cells/$CD4^+CD25^+$ cells/APC (1:1:0.1) were cultured 1:1stored supernatant: fresh culture medium in the presence (Ag, CD3) or absence (Ag, non) of anti-CD3 mAb. Proliferative responses were analyzed at day 4.

that the defective function of $CD4^+CD25^+$ Treg cells following PPD stimulation was not dependent on soluble factors released from T cells and APCs.

Activated $CD4^+CD25^+$ Treg cells suppress the function of PPD-stimulated $CD4^+CD25^-$ effector T cells

Two possibilities could explain the lack of effect of PPD-stimulated $CD4^+CD25^+$ Treg cells on the function of $CD4^+$ $CD25^-$ T cells. First, that activated $CD4^+CD25^+$ Treg cells fail to suppress the function of $CD4^+CD25^-$ T cells by mycobacterial antigens, and second that $CD4^+CD25^+$ Treg cells are not activated by mycobacterial antigens at the late stage of infection. To investigate these possibilities, we purified $CD4^+CD25^+$ T cells from chronically infected mice with BCG or *M. tuberculosis*, then activated *in vitro* with anti-CD3/CD28 mAb-coated beads in the presence of recombinant IL-2. The cells were then cultured with $CD4^+CD25^-$ T cells derived from BCG- or *M. tuberculosis*-infected mice in the presence of PPD. We found that activated $CD4^+CD25^+$ T cells unequivocally suppressed both proliferation and production of IFN-gamma of $CD4^+CD25^-$ T cells stimulated with PPD (Figs 9 and 10). Thus, our data show that both BCG and *M. tuberculosis* infection activate antigen-specific $CD4^+CD25^-$ effector T cells, but not $CD4^+CD25^+$ Treg cells, at the late stage of infection.

Discussion

$CD4^+CD25^+$ Treg cells play a pivotal role in self-tolerance and autoimmune diseases and also in the progression of infectious diseases. It has been shown that $CD4^+CD25^+$ Treg cells are preventive against eradication of persistent pathogens, such as *Leishmania* protozoa, herpes simplex virus and HIV (17–20). Mycobacteria are major parasitic bacteria for eukaryotes (28). In this study, we investigated the role of $CD4^+CD25^+$ Treg cells in mycobacteria infection in mice.

We first studied the effects of Treg cell depletion against infection of mycobacteria. At the early stage of infection, depletion of $CD25^+$ cells significantly suppressed the growth of virulent *M. tuberculosis* strains, such as Kurono and Erdman, suggesting a role for $CD4^+CD25^+$ Treg cells in exacerbation of tuberculosis at the early stage of infection. This is consistent with the previous study performed by Kursar *et al.* (22). This effect of $CD4^+CD25^+$ Treg cells is presumably mediated through naturally occurring $CD4^+CD25^+$ Treg cells, which can be activated through Toll-like receptor (TLR)-mediated signaling (29–32). Mycobacterial DNA [TLR9 ligand (33)] and lipoproteins [TLR2 ligand (34)] may participate in activation of naturally occurring $CD4^+CD25^+$ Treg cells at this stage.

Two to three weeks post-infection, acquired immunity is evident (35). IFN-gamma producing T-helper 1 cells (T_h1) are major effectors in suppressing intracellular survival of

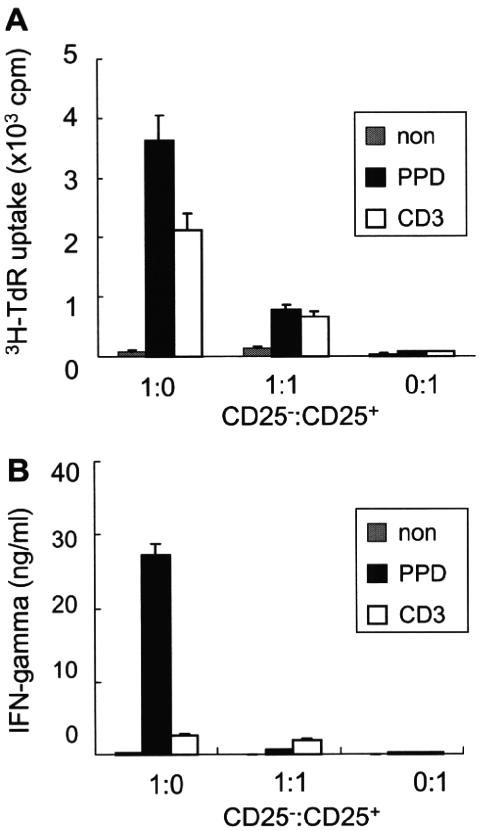

Fig. 9. *In vitro* activation of CD4$^+$CD25$^+$ T cells derived from BCG-infected mice inhibits the function of PPD-stimulated CD4$^+$CD25$^-$ effector T cells. CD4$^+$CD25$^+$ T cells obtained from chronically BCG-infected mice were activated by incubation with anti-CD3/CD28 mAb-coated beads at a bead:cell ratio 2:1 in the presence of 2000 U ml^{-1} of recombinant mouse IL-2 for 48 h. Activated CD4$^+$CD25$^+$ T cells were co-cultured with freshly isolated CD4$^+$CD25$^-$ effector T cells in the presence of PPD (filled column), anti-CD3 mAb (open column) or alone (gray column). (A) Proliferation of CD4$^+$CD25$^-$ effector T cells wase analyzed at day 4. (B) IFN-gamma production in the culture supernatant as measured at day 7.

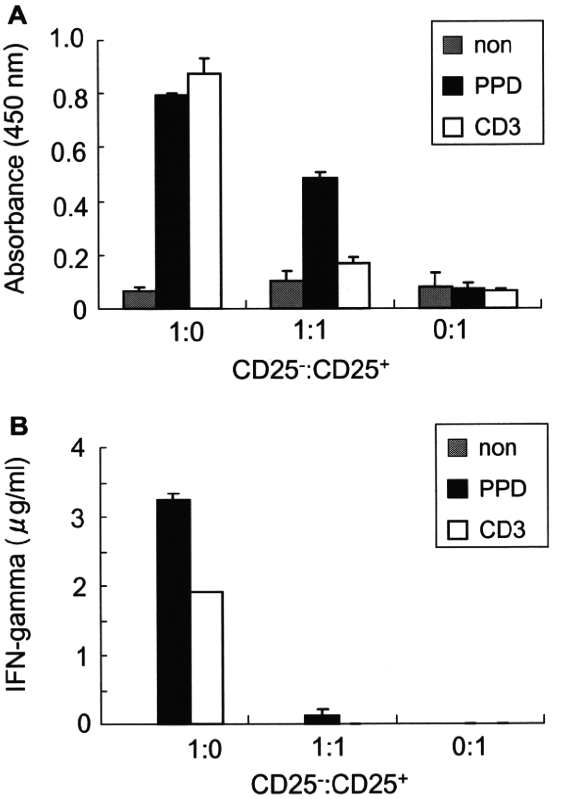

Fig. 10. *In vitro* activation of CD4$^+$CD25$^+$ T cells derived from *Mycobacterium tuberculosis*-infected mice inhibit the function of PPD-stimulated CD4$^+$CD25$^-$ effector T cells. CD4$^+$CD25$^+$ T cells obtained from chronically *M. tuberculosis* H37Rv-infected mice were activated by incubation with anti-CD3/CD28 mAb-coated beads at a bead:cell ratio of 2:1 in the presence of 2000 U ml^{-1} of recombinant mouse IL-2 for 48 h. Activated CD4$^+$CD25$^+$ T cells were co-cultured with freshly isolated CD4$^+$CD25$^-$ effector T cells in the presence of PPD (filled column), anti-CD3 mAb (open column) or alone (gray column). (A) Proliferation of CD4$^+$CD25$^-$ effector T cells was analyzed at day 4. (B) IFN-gamma production in the culture supernatant as measured at day 7.

mycobacteria (36–38). In the CD25$^+$ cell-depletion experiments, the advantages of CD25$^+$ cell depletion were diminished 3 and 5 weeks after the challenge of *M. tuberculosis* Erdman and Kurono, respectively (Figs 2 and 3). We also found that persistence of BCG in mice is not altered by depletion of CD25$^+$ cells by 7D4 (data not shown). These data can be explained by the short-action profile of antibodies. However, we could not find any effect of depletion of CD25$^+$ cells at the chronic stage of infection (Fig. 4), when bacterial numbers were sustained at the same level (39). Similar results were obtained using another anti-CD25 mAb PC6C1, which causes significant reduction of the number of persistent *Leishmania major* in mice by suppressing CD4$^+$CD25$^+$ Treg cells (personal communication with Dr Alan Sher). Furthermore, our *in vivo* experiments in reconstituted SCID mice further suggest that the role of CD4$^+$CD25$^+$ Treg is minimal after infection is established (Fig. 5). The survival kinetics of mice reconstituted with CD4$^+$CD25$^-$ T cells alone are comparable to those in mice reconstituted with both CD4$^+$CD25$^-$ effector T cells and CD4$^+$CD25$^+$ Treg cells (10:1). These data indicate that CD4$^+$CD25$^+$ Treg cells have no impact on the overall outcome of *M. tuberculosis* infection. Kursar *et al.* suggested that CD4$^+$CD25$^+$ Treg cells prevent the bactericidal immune response based on data analyzed in RAG-KO mice reconstituted with each T cell subset (22). However, they reconstituted mice with T cells from naive animals at an unphysiological ratio of CD4$^+$CD25$^-$ T cells to CD4$^+$CD25$^+$ T cells (2:1). These differences may explain the discrepancy between studies.

In order to elucidate the cellular mechanisms of the minimal effect of CD4$^+$CD25$^+$ Treg cells in *M. tuberculosis* infection after the infection was established, we evaluated the function of CD4$^+$CD25$^+$ Treg cells *in vitro*. We activated each population of CD4$^+$ T cells derived from naive and BCG- or *M. tuberculosis*-chronically infected mice with anti-CD3 mAb or *M. tuberculosis*-derived antigens, PPD. BCG has >99.5% identical genome with that of *M. tuberculosis* (40) and therefore BCG and *M. tuberculosis* share almost identical antigens. CD4$^+$CD25$^+$ T cells suppressed anti-CD3-induced

activation (proliferation, production of IFN-gamma and IL-10) of $CD4^+CD25^-$ effector T cells whereas, reflecting our *in vivo* data, PPD stimulation failed to suppress the function of $CD4^+CD25^-$ effector T cells. Both $CD4^+CD25^-$ and $CD4^+CD25^+$ T cells consume IL-2 to proliferate or maintain the state but only $CD25^+CD25^-$ effector T cells produce IL-2. Thus, the level of IL-2 inversely correlated with the number of $CD4^+CD25^+$ T cells (Fig. 6G, H and d) is considered the results of consumption of IL-2 by $CD4^+CD25^+$ T cells but not functional suppression.

One of mechanisms of diminished Treg cell function is mediated by IL-6, which is produced by activated APC through TCR signaling (27). We observed obvious production of IL-6 with PPD stimulation, although which cells produced IL-6 was unknown (Fig. 6, I, J and e). However, neither IL-6 nor other soluble factors released from cells were involved in the non-functional property of $CD4^+CD25^+$ Treg cells following PPD stimulation (Fig. 8). An explanation for this phenomenon is that PPD-specific $CD4^+CD25^+$ Treg cells are not activated at the late stage of mycobacterial infection because $CD4^+CD25^+$ Treg cells activated by anti-CD3/CD28 suppress the function of $CD4^+CD25^-$ effector T cells following stimulation with PPD (Figs 9 and 10).

With the exception of one recent study on herpes simplex virus infection (41), $CD4^+CD25^+$ Treg cells are thought to support parasite persistence in the host by inhibiting the function of effector T cells by a variety of mechanisms. According to this theory, several reports regarding mycobacterial infection have suggested a role for $CD4^+CD25^+$ Treg cells in disease progression and establishment of latent infection (22, 25, 42). However, our findings refute this theory, because $CD4^+CD25^+$ cells did not affect the total infectious load of *M. tuberculosis* in mice (Fig. 5) and mycobacterial infection did not activate mycobacteria-specific $CD4^+CD25^+$ Treg cells (Figs 6, 9 and 10). Several reports showed that FoxP3-positive Treg cells are found in the site of infection with BCG or *M. tuberculosis* (23, 25, 42). However, we consider that these Treg cells are unresponsive to mycobacterial antigens, rather than responding to self-antigens in the disrupted tissues of the infectious legion (43).

In contrast, $CD4^+CD25^+$ Treg cells responding to parasite antigens are activated during infection of *Leishmania* (17, 44) and *Plasmodium* (21). These parasites more closely resemble mammals in the history of evolution; therefore, it can be speculated that they express antigens similar to mammalian self-antigens, which leads to activation of self-antigen-reactive $CD4^+CD25^+$ Treg cells (43). This may be a possible reason for the discrepancy of the host response to mycobacteria versus protozoa. The host must recognize pathogens to survive and mycobacteria represent major bacterial pathogens for vertebrates. In our study, the fact that effector T cells are activated in response to mycobacterial antigens, while suppressive $CD4^+CD25^+$ Treg cells are comparatively silent, is rational based on the host's need to protect itself from mycobacterial infection.

Funding

Japan Health Sciences Foundation; Ministry of Health, Labour and Welfare (Research on Emerging and Re-emerging Infectious Diseases, Health Sciences Research Grants); Ministry of Education, Culture, Sports, Science and Technology; Osaka City University Urban Research; Biochemical Tokyo Research Foundation, and The United States-Japan Cooperative Medical Science Program Against Tuberculosis Leprosy.

Acknowledgements

We would like to thank Dr Toshiki Tamura and Dr Hidefumi Kojima for their advice and Mr Satoru Iwatani for technical support of FACS analysis. We also thank Dr Saburo Yamamoto and Miss Sara Matsumoto for heartfelt encouragement. The authors have no conflicting financial interests.

References

1 Dye, C., Scheele, S., Dolin, P., Pathania, V. and Raviglione, M. C. 1999. Consensus statement. Global burden of tuberculosis: estimated incidence, prevalence, and mortality by country. WHO Global Surveillance and Monitoring Project. *JAMA* 282:677.
2 Jouanguy, E., Altare, F., Lamhamedi, S. *et al.* 1996. Interferon-gamma-receptor deficiency in an infant with fatal bacille Calmette-Guerin infection. *N. Engl. J. Med.* 335:1956.
3 Newport, M. J., Huxley, C. M., Huston, S. *et al.* 1996. A mutation in the interferon-gamma-receptor gene and susceptibility to mycobacterial infection. *N. Engl. J. Med.* 335:1941.
4 Sakaguchi, S. 2000. Regulatory T cells: key controllers of immunologic self-tolerance. *Cell* 101:455.
5 Sakaguchi, S. 2004. Naturally arising CD4+ regulatory t cells for immunologic self-tolerance and negative control of immune responses. *Annu. Rev. Immunol.* 22:531.
6 Shevach, E. M. 2001. Certified professionals: CD4(+)CD25(+) suppressor T cells. *J. Exp. Med.* 193:F41.
7 Read, S., Malmstrom, V. and Powrie, F. 2000. Cytotoxic T lymphocyte-associated antigen 4 plays an essential role in the function of CD25(+)CD4(+) regulatory cells that control intestinal inflammation. *J. Exp. Med.* 192:295.
8 Takahashi, T., Tagami, T., Yamazaki, S. *et al.* 2000. Immunologic self-tolerance maintained by CD25(+)CD4(+) regulatory T cells constitutively expressing cytotoxic T lymphocyte-associated antigen 4. *J. Exp. Med.* 192:303.
9 Shimizu, J., Yamazaki, S., Takahashi, T., Ishida, Y. and Sakaguchi, S. 2002. Stimulation of CD25(+)CD4(+) regulatory T cells through GITR breaks immunological self-tolerance. *Nat. Immunol.* 3:135.
10 McHugh, R. S., Whitters, M. J., Piccirillo, C. A. *et al.* 2002. CD4(+)CD25(+) immunoregulatory T cells: gene expression analysis reveals a functional role for the glucocorticoid-induced TNF receptor. *Immunity* 16:311.
11 Hori, S., Nomura, T. and Sakaguchi, S. 2003. Control of regulatory T cell development by the transcription factor Foxp3. *Science* 299:1057.
12 Sakaguchi, S., Yamaguchi, T., Nomura, T. and Ono, M. 2008. Regulatory T cells and immune tolerance. *Cell* 133:775.
13 Asseman, C., Mauze, S., Leach, M. W., Coffman, R. L. and Powrie, F. 1999. An essential role for interleukin 10 in the function of regulatory T cells that inhibit intestinal inflammation. *J. Exp. Med.* 190:995.
14 Gorelik, L. and Flavell, R. A. 2000. Abrogation of TGFbeta signaling in T cells leads to spontaneous T cell differentiation and autoimmune disease. *Immunity* 12:171.
15 Takahashi, T., Kuniyasu, Y., Toda, M. *et al.* 1998. Immunologic self-tolerance maintained by CD25+CD4+ naturally anergic and suppressive T cells: induction of autoimmune disease by breaking their anergic/suppressive state. *Int. Immunol.* 10:1969.
16 Thornton, A. M. and Shevach, E. M. 1998. CD4+CD25+ immunoregulatory T cells suppress polyclonal T cell activation *in vitro* by inhibiting interleukin 2 production. *J. Exp. Med.* 188:287.
17 Belkaid, Y., Piccirillo, C. A., Mendez, S., Shevach, E. M. and Sacks, D. L. 2002. CD4+CD25+ regulatory T cells control Leishmania major persistence and immunity. *Nature* 420:502.
18 Suvas, S., Kumaraguru, U., Pack, C. D., Lee, S. and Rouse, B. T. 2003. CD4+CD25+ T cells regulate virus-specific primary and memory CD8+ T cell responses. *J. Exp. Med.* 198:889.

19 Aandahl, E. M., Michaelsson, J., Moretto, W. J., Hecht, F. M. and Nixon, D. F. 2004. Human CD4+ CD25+ regulatory T cells control T-cell responses to human immunodeficiency virus and cytomegalovirus antigens. *J. Virol.* 78:2454.

20 Lundgren, A., Suri-Payer, E., Enarsson, K. *et al.* 2003. Helicobacter pylori-specific $CD4^+$ CD25high regulatory T cells suppress memory T-cell responses to H. pylori in infected individuals CD4 T cell activation by myelin oligodendrocyte glycoprotein is suppressed by adult but not cord blood $CD25^+$ T cells. *Infect. Immun.* 71:1755.

21 Hisaeda, H., Maekawa, Y., Iwakawa, D. *et al.* 2004. Escape of malaria parasites from host immunity requires $CD4^+$ $CD25^+$ regulatory T cells. *Nat. Med.* 10:29.

22 Kursar, M., Koch, M., Mittrucker, H. W. *et al.* 2007. Cutting Edge: regulatory T cells prevent efficient clearance of Mycobacterium tuberculosis. *J. Immunol.* 178:2661.

23 Quinn, K. M., McHugh, R. S., Rich, F. J. *et al.* 2006. Inactivation of CD4+ CD25+ regulatory T cells during early mycobacterial infection increases cytokine production but does not affect pathogen load. *Immunol. Cell Biol.* 84:467.

24 Quinn, K. M., Rich, F. J., Goldsack, L. M. *et al.* 2008. Accelerating the secondary immune response by inactivating CD4(+)CD25(+) T regulatory cells prior to BCG vaccination does not enhance protection against tuberculosis. *Eur. J. Immunol.* 38:695.

25 Scott-Browne, J. P., Shafiani, S., Tucker-Heard, G. *et al.* 2007. Expansion and function of Foxp3-expressing T regulatory cells during tuberculosis. *J. Exp. Med.* 204:2159.

26 Kaneko, H., Yamada, H., Mizuno, S. *et al.* 1999. Role of tumor necrosis factor-alpha in *Mycobacterium*-induced granuloma formation in tumor necrosis factor-alpha-deficient mice. *Lab. Invest.* 79:379.

27 Pasare, C. and Medzhitov, R. 2003. Toll pathway-dependent blockade of CD4+CD25+ T cell-mediated suppression by dendritic cells. *Science* 299:1033.

28 Flynn, J. L. and Chan, J. 2001. Immunology of tuberculosis. *Annu. Rev. Immunol.* 19:93.

29 Caramalho, I., Lopes-Carvalho, T., Ostler, D., Zelenay, S., Haury, M. and Demengeot, J. 2003. Regulatory T cells selectively express toll-like receptors and are activated by lipopolysaccharide. *J. Exp. Med.* 197:403.

30 Crellin, N. K., Garcia, R. V., Hadisfar, O., Allan, S. E., Steiner, T. S. and Levings, M. K. 2005. Human CD4+ T cells express TLR5 and its ligand flagellin enhances the suppressive capacity and expression of FOXP3 in CD4+CD25+ T regulatory cells. *J. Immunol.* 175:8051.

31 Peng, G., Guo, Z., Kiniwa, Y. *et al.* 2005. Toll-like receptor 8-mediated reversal of CD4+ regulatory T cell function. *Science* 309:1380.

32 Sutmuller, R. P., den Brok, M. H., Kramer, M. *et al.* 2006. Toll-like receptor 2 controls expansion and function of regulatory T cells. *J. Clin. Invest.* 116:485.

33 Bafica, A., Scanga, C. A., Feng, C. G., Leifer, C., Cheever, A. and Sher, A. 2005. TLR9 regulates Th1 responses and cooperates with TLR2 in mediating optimal resistance to *Mycobacterium tuberculosis*. *J. Exp. Med.* 202:1715.

34 Thoma-Uszynski, S., Stenger, S., Takeuchi, O. *et al.* 2001. Induction of direct antimicrobial activity through mammalian toll-like receptors. *Science* 291:1544.

35 North, R. J. and Jung, Y. J. 2004. Immunity to tuberculosis. *Annu. Rev. Immunol.* 22:599.

36 Flynn, J. L., Chan, J., Triebold, K. J., Dalton, D. K., Stewart, T. A. and Bloom, B. R. 1993. An essential role for interferon gamma in resistance to *Mycobacterium tuberculosis* infection. *J. Exp. Med.* 178:2249.

37 Cooper, A. M., Dalton, D. K., Stewart, T. A., Griffin, J. P., Russell, D. G. and Orme, I. M. 1993. Disseminated tuberculosis in interferon gamma gene-disrupted mice. *J. Exp. Med.* 178:2243.

38 Scanga, C. A., Mohan, V. P., Yu, K. *et al.* 2000. Depletion of CD4(+) T cells causes reactivation of murine persistent tuberculosis despite continued expression of interferon gamma and nitric oxide synthase 2. *J. Exp. Med.* 192:347.

39 Jung, Y. J., LaCourse, R., Ryan, L. and North, R. J. 2002. Evidence inconsistent with a negative influence of T helper 2 cells on protection afforded by a dominant T helper 1 response against Mycobacterium tuberculosis lung infection in mice. *Infect. Immun.* 70:6436.

40 Behr, M. A., Wilson, M. A., Gill, W. P. *et al.* 1999. Comparative genomics of BCG vaccines by whole-genome DNA microarray. *Science* 284:1520.

41 Lund, J. M., Hsing, L., Pham, T. T. and Rudensky, A. Y. 2008. Coordination of early protective immunity to viral infection by regulatory T cells. *Science* 320:1220.

42 Roberts, T., Beyers, N., Aguirre, A. and Walzl, G. 2007. Immunosuppression during active tuberculosis is characterized by decreased interferon- gamma production and CD25 expression with elevated forkhead box P3, transforming growth factor-beta, and interleukin-4 mRNA levels. *J. Infect. Dis.* 195:870.

43 Nishikawa, H., Kato, T., Tawara, I. *et al.* 2005. Definition of target antigens for naturally occurring CD4(+) CD25(+) regulatory T cells. *J. Exp. Med.* 201:681.

44 Mendez, S., Reckling, S. K., Piccirillo, C. A., Sacks, D. and Belkaid, Y. 2004. Role for CD4(+) CD25(+) regulatory T cells in reactivation of persistent leishmaniasis and control of concomitant immunity. *J. Exp. Med.* 200:201.

Biochemical and Biophysical Research Communications 392 (2010) 277–282

Contents lists available at ScienceDirect

Biochemical and Biophysical Research Communications

journal homepage: www.elsevier.com/locate/ybbrc

Genetic immunization based on the ubiquitin-fusion degradation pathway against *Trypanosoma cruzi*

Bin Chou [a,b], Kenji Hiromatsu [a,*], Hajime Hisaeda [b], Xuefeng Duan [b], Takashi Imai [b], Shigeo Murata [c], Keiji Tanaka [c], Kunisuke Himeno [b]

[a] Department of Microbiology and Immunology, Faculty of Medicine, Fukuoka University, 7-45-1 Nanakuma, Jonan-ku, Fukuoka 814-0180, Japan
[b] Department of Parasitology, Graduate School of Medical Science, Kyushu University, Fukuoka 812-8582, Japan
[c] Department of Molecular Oncology, The Tokyo Metropolitan Institute of Medical Science, Tokyo 113-8613, Japan

ARTICLE INFO

Article history:
Received 15 December 2009
Available online 7 January 2010

Keywords:
Amastigote surface protein-2
Trypanosoma cruzi
DNA vaccine
Ubiquitin-fusion degradation

ABSTRACT

Cytotoxic CD8$^+$ T cells are particularly important to the development of protective immunity against the intracellular protozoan parasite, *Trypanosoma cruzi*, the etiological agent of Chagas disease. We have developed a new effective strategy of genetic immunization by activating CD8$^+$ T cells through the ubiquitin-fusion degradation (UFD) pathway. We constructed expression plasmids encoding the amastigote surface protein-2 (ASP-2) of *T. cruzi*. To induce the UFD pathway, a chimeric gene encoding ubiquitin fused to ASP-2 (pUB-ASP-2) was constructed. Mice immunized with pUB-ASP-2 presented lower parasitemia and longer survival period, compared with mice immunized with pASP-2 alone. Depletion of CD8$^+$ T cells abolished protection against *T. cruzi* in mice immunized with pUB-ASP-2 while depletion of CD4$^+$ T cells did not influence the effective immunity. Mice deficient in LMP2 or LMP7, subunits of immunoproteasomes, were not able to develop protective immunity induced. These results suggest that ubiquitin-fused antigens expressed in antigen-presenting cells were effectively degraded via the UFD pathway, and subsequently activated CD8$^+$ T cells. Consequently, immunization with pUB-ASP-2 was able to induce potent protective immunity against infection of *T. cruzi*.

© 2010 Elsevier Inc. All rights reserved.

Introduction

Trypanosoma cruzi is an intracellular protozoan hemoflagellate parasite of humans and many other mammals. It is also the etiological pathogen of Chagas disease. Patients infected with *T. cruzi* have been treated with many kinds of drugs, but those therapies are hardly effective in chronically infected individuals. Furthermore, parasites that are naturally resistant to chemotherapy have been reported in various regions of Latin America [1].

T cell-mediated immunity, especially via CD8$^+$ cytotoxic T lymphocytes (CTL), has been demonstrated to play a crucial role in resolving *T. cruzi* infection in humans and mice [2]. Antigens recognized by CD8$^+$ T cells are first processed by the ubiquitin proteasome system (UPS) [3]. CD8$^+$ T cells then recognize antigenic epitopes presented by major histocompatibility complex (MHC) class I molecules on the surface of infected host cells. As a result, *T. cruzi* is cleared by cytolysis of parasite-infected host cells [4]. Activation of CD8$^+$ T cells requires antigen-processing through the UPS prior to presentation in association with MHC class I molecules [5].

Recently, it was reported that an artificially fused mono-ubiquitin and antigenic protein was readily directed to the proteasome, and those antigenic peptides are then effectively presented on antigen-presenting cells (APCs). This virtual pathway of UPS was named the ubiquitin-fusion degradation (UFD) pathway [6]. This immunization strategy is effective in maximizing CD8$^+$ T cell-responses against those antigenic peptides. We previously reported that immunization with naked DNA encoding an antigen artificially fused to a mono-ubiquitin is an efficient strategy for the induction of antigen-specific immunity mediated by CD8$^+$ T cells [7].

A number of antigens of *T. cruzi* recognized by the immune system have been defined at the molecular level in the last decade [8,9]. Genetic immunization strategies have recently become popular and attractive for prophylaxis and therapy against infection of *T. cruzi*. It has been shown that amastigote surface protein-2 (ASP-2) is one of the targets for CD8$^+$ T cells and contains CTL epitopes such as the H-2K^b restricted VNHRFTLV [10]. Based on these facts, we developed a new strategy for genetic immunization employing

Abbreviations: *T. cruzi*, *Trypanosoma cruzi*; UFD, ubiquitin-fusion degradation; ASP-2, amastigote surface protein-2; UPS, ubiquitin proteasome system

* Corresponding author. Fax: +81 92 801 9390.
E-mail address: khiromatsu@fukuoka-u.ac.jp (K. Hiromatsu).

0006-291X/$ - see front matter © 2010 Elsevier Inc. All rights reserved.
doi:10.1016/j.bbrc.2009.12.166

the UFD pathway. Expression plasmids encoding ASP-2 fused to a mono-ubiquitin (pUB-ASP-2) were constructed. Mice immunized with pUB-ASP-2 exhibited a low parasitemia and survived longer compared with mice in the control group; while immunization with pASP-2 alone was scarcely effective. $CD8^+$ T cells exerted ASP-2 specific cytotoxic activities and IFN-γ secretion. Application of the UFD pathway for genetic immunization was confirmed by using immunoproteasome deficient mice such as PA28α/β, LMP2 or LMP7 KO mice.

Materials and methods

Animals and parasites. Female 8-week old C57BL/6 (B6) mice were purchased from Seac Yoshitomi (Fukuoka, Japan). Proteasome activator PA28 knockout ($PA28\alpha/\beta^{-/-}$) and immunoproteasome subunit LMP2 or LMP7 knockout ($LMP2^{-/-}$ or $LMP7^{-/-}$) mice were B6 background. The Tulahuen strain of *T. cruzi* was maintained by weekly passage in B6 mice.

Cloning and sequencing. Total RNA was isolated from liver sections obtained from *T. cruzi* infected B6 mice and reverse-transcribed to cDNA. ASP-2 cDNA was amplified by PCR using sense, 5′-ATGCTCTCACGTGTTGCTGCTGTC-3′, and antisense 5′-TTA GTCGCCACCGTTTCCTTTTTTATCG-3′ primers. Specific oligonucleotides were designed on the basis of the previously published nucleotide sequence of *asp-2* [11]. The resulting amplicon was ligated into a pGEM-T easy vector (Promega, USA) and transformed into DH5α *Escherichia coli* (Invitrogen, USA). Clones containing inserts of the expected size were selected. Sequencing was initially performed using SP6 and T 7 primers, the sequences of which were present in the flanking regions of the pGEM-T easy vector. Subsequently, to complete sequencing of each clone, new oligonucleotides were designed to cover the entire sequence.

DNA and predicted amino acid sequences were analyzed using the Lasergene 7.1 software package (DNASTAR Inc., USA). Sequence alignments were produced using Clustal V. Analysis for potential secretory signal peptides (SP) was performed at the SignalP website (http://www.cbs.dtu.dk/services/SignalP/).

Plasmids. A plasmid encoding ASP-2 (aa65–703, signal peptide deleted) and tagged with His residues (pASP-2) was constructed by amplifying *asp-2* from clone 2 using the following primers: 5′-GCATCCTCGAGATGGCTGTGGAGGGTAAGTCCGGG-3′, 5′-GTCATCTTAAGTTAGTGATGGTGGTGATGGTGGTCGCCACCGTTTCCTTTTTTATCG-3′. PCR products were treated with enzymes and inserted into the XhoI and AflII sites of the pcDNA3.1(−) vector (Invitrogen, USA). The pUB vector we made previously was used to construct pUB-ASP-2 (aa65–703, SP deleted) and tagged with His [7]. The gene *asp-2*, was cut from pASP-2 and inserted into the XhoI and AflII sites of the pUB vector.

In vivo gene transfer and challenge of T. cruzi. As described previously, a Helios Gene Gun (BioRad, USA) was used [12]. Protocols of immunization and infection with *T. cruzi* trypomastigotes were same with previous description [12].

In vitro transfection and Western blotting. Protocols of transfection and Western immunoblotting were same as described previously [12,13].

Cytotoxicity assay, ELISA and flow cytometry. Protocols of cytotoxicity assay, ELISA and flow cytometry were same as described previously [12,13].

Statistical analysis. Data are expressed as mean ± SEM. Differences between experimental groups within each experiment were analyzed by using the unpaired Student's *t*-test and were considered significant when the *p*-value was <0.05. Survival differences between experimental groups within each experiment were analyzed by using the log-rank test and were considered significant when the *p*-value was <0.05.

Results

Construction of plasmids encoding ASP-2 or UB-ASP-2

The *asp-2* gene is polymorphic, as its sequence is different even in the same strains of *T. cruzi* [14]. In this study, we obtained four clones of the *asp-2* gene from the Tulahuen strain and picked up one particular clone (clone 2: GenBank Accession No. GU445326). Compared with the original sequence of the Brazil strain (GenBank Accession No. U77951) and the sequence of the Tulahuen strain (GenBank Accession No. EF579921), the amino acid sequence of ASP-2 used in this study contained the ASP box motif (SxDxGxTW) and the VTV box motif (VTVxNVxLYNR) (Fig. 1A). The amino acid identity of ASP-2 used in this study compared with the Brazil strain is 89.8%, and 83.1% when compared with the Tulahuen strain. The H-$2K^b$ restricted CTL epitope (aa553–560, VNHSFTLV) contains a single amino acid change when compared with the Brazil strain [15], and two amino acid changes when compared with the Tulahuen strain [14]. ASP-2 and UB-ASP-2 expression plasmids were constructed as described in the materials and methods section (Fig. 1B). Construction of pASP-2 and pUB-ASP-2 was confirmed by DNA sequencing. The expression of ASP-2 or the fusion protein UB-ASP-2 was confirmed by Western immunoblotting after transfection of COS7 cells with these plasmids; a specific band was detected in lysates from cells transfected with pASP-2 or pUB-ASP-2 (Fig. 1C).

Anti-parasite immunity against T. cruzi was induced by immunization with pUB-ASP-2

CTL epitopes are produced through the ubiquitin–proteasome pathway and we expected that antigen presentation of MHC class I-associated ASP-2 peptides to $CD8^+$ T cells would become significantly more efficient following immunization with pUB-ASP-2. To verify this, B6 mice were immunized with pcDNA, pASP-2 or pUB-ASP-2 into the abdominal skin by using a gene-gun system four times, at two-week intervals. Two weeks following the last immunization, mice were challenged with 1000 blood-derived *T. cruzi* trypomastigotes by subcutaneous injection at the base of the tail. Mice immunized with pUB-ASP-2 developed a lower parasitemia than control pcDNA immunized groups (Fig. 2A); survival was also prolonged by immunization with pUB-ASP-2 (Fig. 2B). Six out of seven pUB-ASP-2 immunized mice survived until the end of the experiment. Mice immunized with pASP-2 did not develop a protective response suggesting that artificial fusion of the gene encoding mono-ubiquitin and the ASP-2 protein was required for the induction of immunity.

Immune response following immunization with pUB-ASP-2

To investigate the mechanism of protective immunity conferred by immunization with pUB-ASP-2, spleen cells separated from mice immunized with pcDNA, pASP-2 or pUB-ASP-2, were co-cultured with the non-specific stimulator PMA. Production of intracellular IFN-γ and Granzyme b (GZM-b) by T cells was analyzed using flow cytometry. Intracellular IFN-γ and GZM-b was strongly induced in $CD8^+$ T cells of mice immunized with pUB-ASP-2 (Fig. 3A). The absolute number of both IFN-γ^+CD8^+ T cells and GZM-b^+CD8^+ T cells in the spleen was significantly higher in pUB-ASP-2 immunized mice (Fig. 3B). There was no significant difference in the IFN-γ and GZM-b secretion level of $CD4^+$ T cells. Production of IFN-γ and GZM-b in $CD4^+$ T cells was at almost the same level in mice treated with pcDNA, pASP-2 or pUB-ASP-2 (data not shown). These results indicate that immunization with pUB-ASP-2 promotes $CD8^+$ T cell activation, and enhances the expression level of IFN-γ and GZM-b in $CD8^+$ T cells.

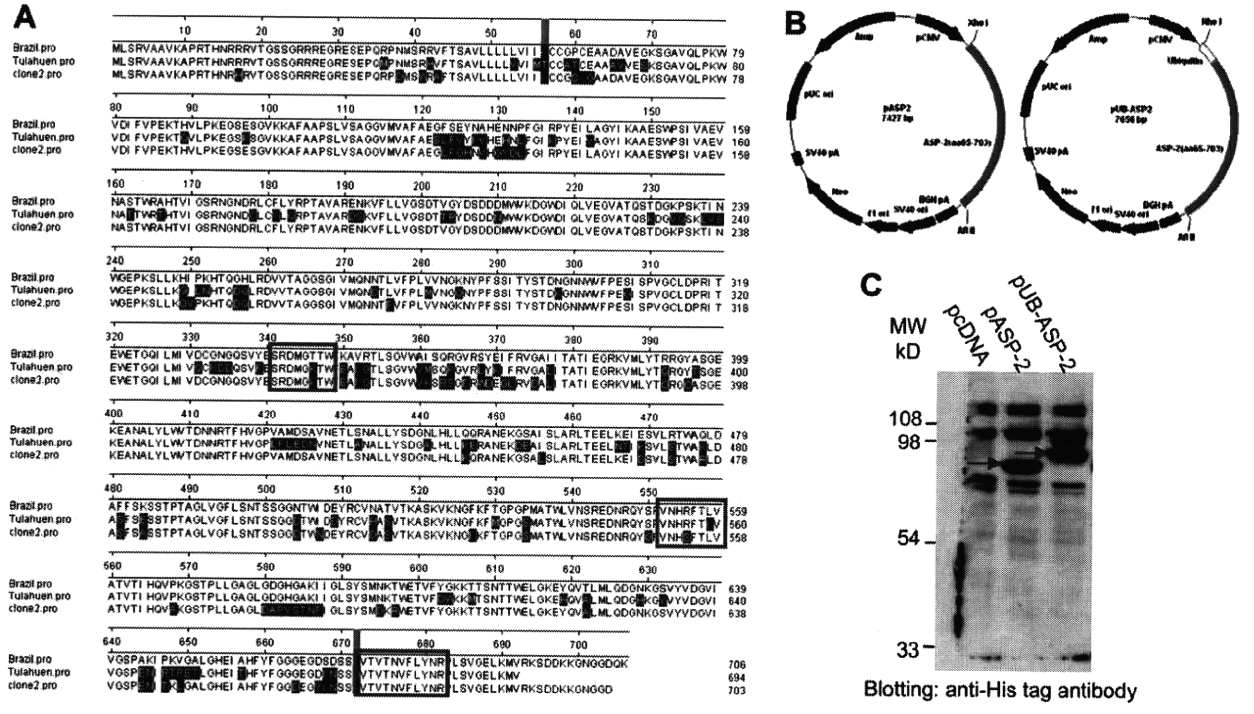

Fig. 1. Sequence of ASP-2, plasmid construction and expression *in vivo*. (A) Predicted amino acid sequence of ASP-2 clone 2 (GenBank Accession No. GU445326) and comparison with predicted amino acid sequences of Brazil (GenBank Accession No. U77951) and Tulahuen (GenBank Accession No. EF579921) strains. Letters marked in red are different from the original sequence of the Brazil strain. Letters highlighted in blue indicate the ASP box motif (SxDxGxTW) and the VTV box motif (VTVxNVxLYNR). Letters highlighted with a red box indicate the H-2K^b restricted CTL epitope. (B) Schematic representation of pASP-2 (upper panel) and pUB-ASP-2 (lower panel). (C) Expression of ASP-2 or UB-ASP-2 in COS7 cells. Sizes of the molecular weight markers are shown on the left.

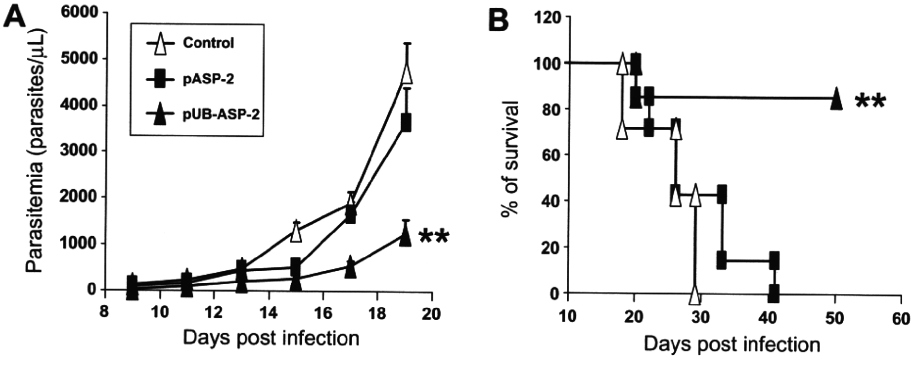

Fig. 2. Induction of anti-parasite immunity by immunization with pUB-ASP-2. C57BL/6 mice were immunized with pcDNA (open triangles), pASP-2 (closed squares) or pUB-ASP-2 (closed triangles), and then challenged with 1000 blood-derived *T. cruzi* trypomastigotes. Mice were scored on the basis of parasitemia (A) and survival (B). (A) Each value represents the mean ± SEM from seven mice in each group. $^{**}p < 0.02$ compared with other groups by the Student's *t*-test. (B) Results are expressed as the percentages of surviving mice in groups of seven. $^{**}p < 0.02$ compared with other groups by the log-rank test.

Antigen-specific CD8$^+$ T cells are activated by immunization with pUB-ASP-2

To confirm that these activated CD8$^+$ T cells were specific to ASP-2, we cultured splenocytes with the ASP-2 CTL epitope (VNHSFTLV) and then measured the production of IFN-γ and GZM-b by performing intracellular FACS. As expected, the percentage and absolute cell number of IFN-γ$^+$ or GZM-b$^+$ CD8$^+$ T cells in pUB-ASP-2 immunized mice were significantly higher than in mice immunized with pcDNA or pASP-2 (Fig. 3C and D). No differences in production of IFN-γ and GZM-b were seen in CD4$^+$ T cells between the control and immunized mice (data not shown).

The amount of secreted IFN-γ in supernatants from spleen cells stimulated with the ASP-2 epitopes was measured by ELISA. The production of IFN-γ in the supernatant from mice immunized with pUB-ASP-2 was significantly higher than those from mice immunized with pcDNA or pASP-2 (Fig. 3E).

To clarify the ASP-2 specific cytotoxic activity of CD8$^+$ T cells, we examined the CTL activity of CD8$^+$ T cells isolated from mice immunized with pUB-ASP-2. Compared with other immunized groups, CTL activities of CD8$^+$ T cells isolated from mice immunized with pUB-ASP-2 were prominent in H-2^b-bearing EL4 cells pulsed with ASP-2 epitopes (Fig. 3F). This clearly demonstrated that ASP-2 specific CD8$^+$ T cells were specifically activated by immunization with pUB-ASP-2.

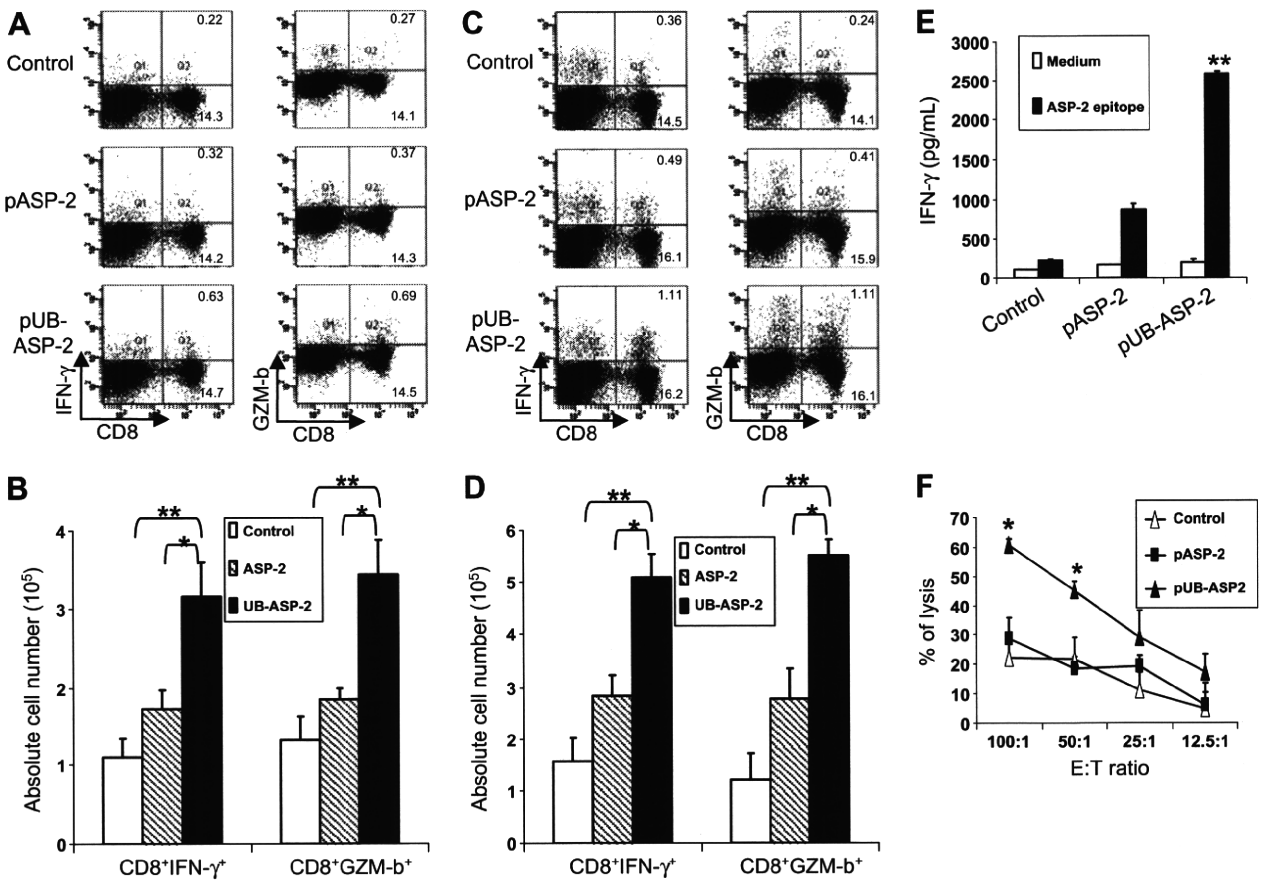

Fig. 3. Functional analysis of splenocytes in mice immunized with pUB-ASP-2. Immunized mice were sacrificed 10 days after the last booster injection. (A and B) Spleen cells were isolated and re-stimulated with PMA for 4 h *in vitro*. (A) Percentage of IFN-γ or Granzyme b positive cells was measured using a FACScan flow cytometer. (B) Total cell number is also indicated. $^{**}p < 0.02$ compared with control group by the Student's *t*-test. $^{*}p < 0.05$ compared with the pASP-2 group by the Student's *t*-test. (C–F) Spleen cells were isolated and re-stimulated with CTL epitope for 4 days *in vitro*. (C) Percentage of IFN-γ or Granzyme b positive cells was measured using FACScan flow cytometer. (D) Total cell number is also indicated. $^{**}p < 0.02$ compared with control group by the Student's *t*-test. $^{*}p < 0.05$ compared with the pASP-2 group by the Student's *t*-test. (E) IFN-γ secretion in the supernatant was measured. $^{**}p < 0.02$ compared with other groups by the Student's *t*-test. (F) CTL activity of $CD8^+$ T cells was measured. $^{*}p < 0.05$ compared with other groups by the Student's *t*-test.

Anti-parasite immunity induced by pUB-ASP-2 was dependent on $CD8^+$ T cells

To assess the role of $CD8^+$ T cells *in vivo*, we depleted $CD4^+$ or $CD8^+$ T cells by treatment with specific antibodies one day before infection with *T. cruzi*. Mice depleted of $CD8^+$ T cells showed a higher parasitemia compared with control mice (Fig. 4A) and died earlier than mice in other groups (Fig. 4B). $CD4^+$ T cells were not required for the effector phase to clear and resist infection with *T. cruzi* as evaluated by parasitemia and survival rate, indicating the efficiency of immunization with pUB-ASP-2 was solely dependent upon $CD8^+$ T cells *in vivo*. These results are also consistent with what we previously reported regarding a DNA vaccine against *T. cruzi* using TSA-1 as a target gene [12].

Degradation of UB-ASP-2 is dependent on proteasome in vitro

Physical binding between ASP-2 with mono-ubiquitin was crucial for the activation of ASP-2 specific $CD8^+$ T cells. This finding indicates that after artificial binding of mono-ubiquitin to ASP-2, the *ub-asp-2* gene products are rapidly degraded by the proteasome through the UFD pathway. Thus, ASP-2 epitopes are efficiently presented to MHC class I molecules, resulting in effective induction of $CD8^+$ T cells specific for the CTL epitope in ASP-2. These hypotheses were confirmed by our Western immunoblotting results. COS7 cells transfected with plasmids in the presence of the proteasome inhibitor MG-132, significantly repressed degradation of UB-ASP-2 proteins, resulting in an accumulation of UB-ASP-2 proteins (Fig. 4C). There was no difference in the amount of ASP-2 proteins present in cells whether MG-132 was present or absent. As shown in Fig. 4D, normalized to HSP90, the detectable amount of UB-ASP-2 proteins was approximately 40% lower without MG-132. These results clearly indicate that fusion of ASP-2 with a mono-ubiquitin renders the chimeric protein susceptible to degradation via the UFD pathway and the increased production of ASP-2 epitopes via the UFD pathway leads to efficient antigen presentation to $CD8^+$ T cells.

The critical role of the immunoproteasome in induction of protective immunity by pUB-ASP-2

We used mice deficient in the proteasome regulator PA28 complex (α/β) or the immunoproteasome subunits LMP2 or LMP7 to clarify whether induction of anti-parasite immunity by pUB-ASP-2 immunization is dependent on the immunoproteasome through the UFD pathway *in vivo* [16–18]. Protection against *T. cruzi* induced by pUB-ASP-2 was completely abolished in LMP2 or LMP7 knockout (KO) mice. These KO mice immunized with pUB-ASP-2 or pcDNA3.1 had a similar survival rate (Fig. 4E). Survival time was prolonged in PA28α/β KO mice immunized with pUB-ASP-2 after *T. cruzi* infection, but decreased when compared with wild-type mice immunized with pUB-ASP-2 (Fig. 4E). These data indi-

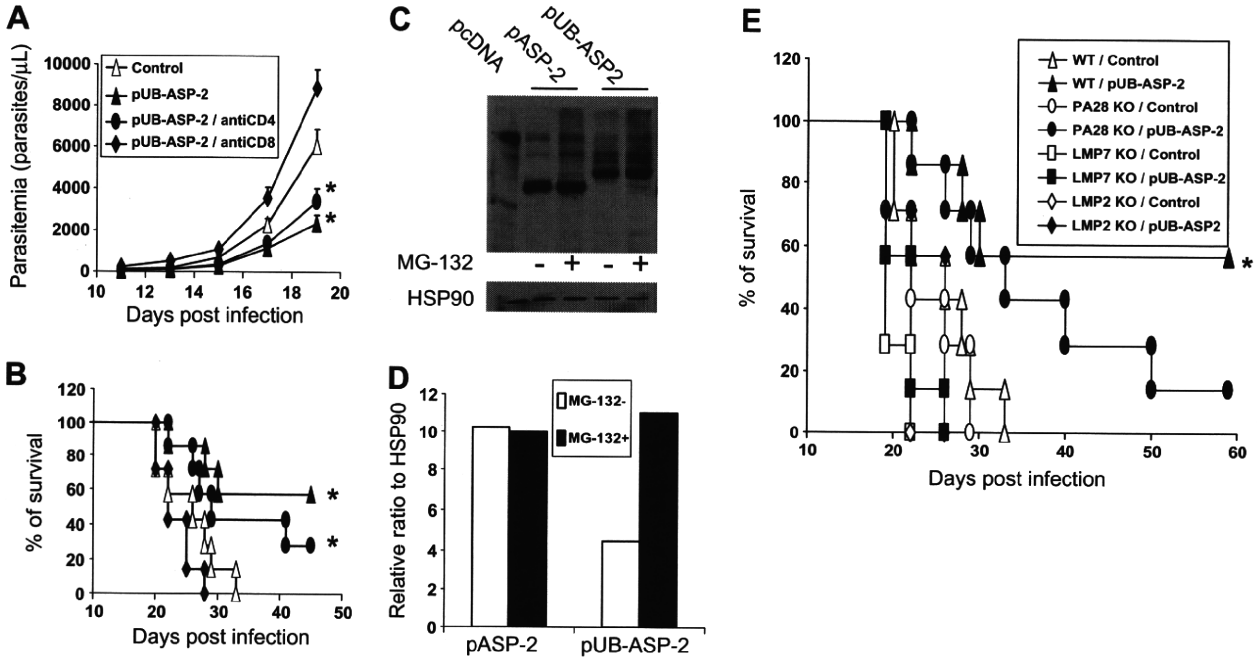

Fig. 4. Effects of immunization with pUB-ASP-2 were dependent on CD8$^+$ T cells *in vivo*; and critical involvement of the proteasome in the processing of UB-ASP-2 proteins *in vitro* and the effect of immunization with pUB-ASP-2 *in vivo*. (A and B) Mice were immunized with pUB-ASP-2 three times and treated with anti-CD4 (500 μg/mice) or anti-CD8 (500 μg/mice) depletion antibodies at one day before the challenge with *T. cruzi*. (A) Parasitemia levels of each group of mice. *$p < 0.05$ compared with the control group by the Student's *t*-test. (B) The survival of each group of mice. *$p < 0.05$ compared with the control group by the log-rank test. (C) COS7 cells transfected with pcDNA3.1(−), pASP-2 or pUB-ASP-2 were cultured with or without MG-132. Cell lysates were used for Western immunoblotting and proteins detected with an anti-His antibody (upper panel) or anti-HSP90 antibody (lower panel). (D) Relative expression to HSP90 was calculated using densitometry. (E) Survival rate of immunoproteasome subunit deficient mice. PA28α/β$^{-/-}$, LMP2$^{-/-}$ and LMP7$^{-/-}$ mice were immunized with the control plasmid pcDNA3.1 or pUB-ASP-2. *$p < 0.05$ compared with the wild type/control group by the log-rank test.

cate that immunoproteasomes play critical roles in producing ASP-2 epitopes and thus activating ASP-2 specific CD8$^+$ T cells by immunization with pUB-ASP-2.

Discussion

CD8$^+$ T cells are important for host resistance against *T. cruzi* infection [2] as they are intracellular protozoan parasites. Many antigenic peptides of *T. cruzi* have been identified as potential vaccine candidates in the last decade [8,9], including the peptides of the *T. cruzi* trans-sialidase family and the trans-sialidase-like family. Trypomastigote surface antigen-1 (TSA-1), a member of the *T. cruzi* trans-sialidase family is expressed on the trypomastigote, but not on the amastigote of *T. cruzi*. In mammalian hosts, *T. cruzi* cycles between extracellular, non-replicative trypomastigotes circulating in the blood and intracellular replicative amastigotes. Extracellular trypomastigote appears to be an inappropriate target for CD8$^+$ T cells since the protozoa itself does not express MHC class I molecules. ASP-2 is a recognized antigen of the intracellular amastigote of *T. cruzi*, and includes the CTL epitopes on APCs. In the present study, we employed ASP-2 as the candidate protein for immunization and inducing specific activated CD8$^+$ T cells.

Endogenous antigens are processed by the proteasome after being polyubiquitinated [5]. This type of antigen processing has been accepted as the ubiquitin–proteasome system (UPS) [3]. Antigenic peptides fused with a mono-ubiquitin will be effectively directed to be poly-ubiquitination and the fusion protein then introduced to the UPS and degraded. This virtual route for the UPS is known as the UFD pathway [6]. Based on this mechanism, we developed a novel immunization strategy to activate antigen-specific CD8$^+$ T cells by inducing the UFD pathway [7]. We constructed the plasmid pUB-ASP-2, encoding the ASP-2 protein fused to a mono-ubiquitin. Using an *in vitro* system, we confirmed that ASP-2 artificially fused with ubiquitin was degraded to a large extent in COS7 cells. The detectable amount of UB-ASP-2 in COS7 cells transfected with pUB-ASP-2 was lower than that of ASP-2 in COS7 cells transfected with pASP-2. In the presence of the proteasome inhibitor, MG-132, the degradation of UB-ASP-2 was inhibited. The detectable amount of UB-ASP-2 in pUB-ASP-2 transfected COS7 cells was similar to the levels of ASP-2 in pASP-2 transfected COS7 cells in the presence of MG-132. In accordance with our previous report [7], the UFD pathway plays a central role in removing the CTL epitopes of ASP-2 by degrading the ubiquitinated ASP-2 protein. Subsequently, those CTL epitopes are directed to MHC class I molecules in the endoplasmic reticulum resulting in the activation of ASP-2-specific CD8$^+$ T cells.

In this study, immunization with a plasmid encoding ASP-2 fused to a mono-ubiquitin, induced a very strong protective immunity against *T. cruzi* infection when compared with immunization with ASP-2 alone. ASP-2 specific CTL activity was induced in mice immunized with pUB-ASP-2, and ASP-2 specific production of IFN-γ and GZM-b in CD8$^+$ T cells were also enhanced compared with pASP-2 immunized mice. This protective immunity was ablated in mice where CD8$^+$ but not CD4$^+$ T cells were depleted. Therefore, application of ASP-2 fused with a mono-ubiquitin appeared to be an efficient strategy to induce a CD8$^+$ T cell mediated immune response against *T. cruzi* by activating the UFD pathway.

The immunomodulatory cytokine IFN-γ, which is mainly secreted by activated CD8$^+$ T cells, Th1 cells and NK cells, enhances antigen presentation by modifying proteasome regulators and subunits, in addition to upregulating MHC and TAP genes. IFN-γ regulates the expression of PA28α and PA28β, which form the heptameric proteasome activator complex PA28 [19]. This heteromultimer is able to bind to the α rings of the 20S core proteasome, enhancing proteolytic activity of the proteasome. Studies *in vitro*

have shown that purified PA28α/β can enhance coordinated dual cleavage of the 20S proteasome, resulting in an augmented output and liberation of peptides [20]. IFN-γ also alters the quality of protease activity in the proteasome by incorporating three IFN-γ inducible catalytic subunits, LMP2, LMP7 and MECL-1, to replace the constitutive catalytic subunits (γ/δ, X/MB1 and Z, respectively) in the 20S core proteasome during biogenesis [21]. The 20S core proteasome incorporating LMP2, LMP7 and MECL-1 is known as the immunoproteasome [3]. This IFN-γ inducible immunoproteasome is more favorable than the constitutive proteasome for antigen presentation as subunits induced by IFN-γ stimulate cleavage of hydrophobic, basic and branched chain residues instead of acidic ones [22,23]. To confirm utilization of the UFD pathway is indispensable for $CD8^+$ T cell induction of protective immunity, mice deficient in immunoproteasome subunits were used. The effects of immunization with pUB-ASP-2 was severely impaired in LMP2/7 KO mice, and partially repressed in PA28α/β KO mice. It was thought that the capacity to generate CTL epitopes of ASP-2 was decreased in PA28α/β KO mice, although our results indicate these epitopes were still generated. Both LMP2 and LMP7 have specific cleavage activity after basic or hydrophobic residues of peptides, therefore LMP2 and LMP7 KO mice should not produce ASP-2 epitopes and consequently not activate $CD8^+$ T cells.

In the present study, we immunized mice with plasmids encoding ASP-2 without a signal peptide to minimize the effects of $CD4^+$ T cells, and to diminish the production of ASP-2 specific antibodies in mice after immunization with plasmids. It is interesting that mice immunized with pUB-ASP-2 and treated with anti-CD4 antibodies are still resistant to *T. cruzi* infection. These data indicate that $CD8^+$ T cell-mediated anti-parasite immunity was induced using a novel immunization strategy without the support of $CD4^+$ T cells. It is appealing to apply this strategy of immunization with HIV patients because their $CD4^+$ T cell function is defective [24].

Acknowledgments

This work was supported by grants-in-aid from the Ministry of Education, Science, Sport and Culture of Japan (15019075, 15025255, 15390136, 15659265).

References

[1] E.L. Camandaroba, E.A. Reis, M.S. Goncalves, M.G. Reis, S.G. Andrade, *Trypanosoma cruzi*: susceptibility to chemotherapy with benznidazole of clones isolated from the highly resistant Colombian strain, Rev. Soc. Bras. Med. Trop. 36 (2003) 201–209.
[2] Z. Brener, R.T. Gazzinelli, Immunological control of *Trypanosoma cruzi* infection and pathogenesis of Chagas' disease, Int. Arch. Allergy Immunol. 114 (1997) 103–110.
[3] K. Tanaka, M. Kasahara, The MHC class I ligand-generating system: roles of immunoproteasomes and the interferon-gamma-inducible proteasome activator PA28, Immunol. Rev. 163 (1998) 161–176.
[4] R.L. Tarleton, L. Zhang, Chagas disease etiology: autoimmunity or parasite persistence?, Parasitol Today 15 (1999) 94–99.
[5] C.M. Pickart, Mechanisms underlying ubiquitination, Annu. Rev. Biochem. 70 (2001) 503–533.
[6] E.S. Johnson, P.C. Ma, I.M. Ota, A. Varshavsky, A proteolytic pathway that recognizes ubiquitin as a degradation signal, J. Biol. Chem. 270 (1995) 17442–17456.
[7] M. Zhang, C. Obata, H. Hisaeda, K. Ishii, S. Murata, T. Chiba, K. Tanaka, Y. Li, M. Furue, B. Chou, T. Imai, X. Duan, K. Himeno, A novel DNA vaccine based on ubiquitin-proteasome pathway targeting 'self'-antigens expressed in melanoma/melanocyte, Gene Ther. 12 (2005) 1049–1057.
[8] V.A. Campo, C.A. Buscaglia, J.M. Di Noia, A.C. Frasch, Immunocharacterization of the mucin-type proteins from the intracellular stage of *Trypanosoma cruzi*, Microbes Infect. 8 (2006) 401–409.
[9] B. Wizel, M. Nunes, R.L. Tarleton, Identification of *Trypanosoma cruzi* trans-sialidase family members as targets of protective CD8+ TC1 responses, J. Immunol. 159 (1997) 6120–6130.
[10] H.P. Low, M.A. Santos, B. Wizel, R.L. Tarleton, Amastigote surface proteins of *Trypanosoma cruzi* are targets for CD8+ CTL, J. Immunol. 160 (1998) 1817–1823.
[11] H.P. Low, R.L. Tarleton, Molecular cloning of the gene encoding the 83 kDa amastigote surface protein and its identification as a member of the *Trypanosoma cruzi* sialidase superfamily, Mol. Biochem. Parasitol. 88 (1997) 137–149.
[12] B. Chou, H. Hisaeda, J. Shen, X. Duan, T. Imai, L. Tu, S. Murata, K. Tanaka, K. Himeno, Critical contribution of immunoproteasomes in the induction of protective immunity against *Trypanosoma cruzi* in mice vaccinated with a plasmid encoding a CTL epitope fused to green fluorescence protein, Microbes Infect. 10 (2008) 241–250.
[13] M. Zhang, K. Ishii, H. Hisaeda, S. Murata, T. Chiba, K. Tanaka, Y. Li, C. Obata, M. Furue, K. Himeno, Ubiquitin-fusion degradation pathway plays an indispensable role in naked DNA vaccination with a chimeric gene encoding a syngeneic cytotoxic T lymphocyte epitope of melanocyte and green fluorescent protein, Immunology 112 (2004) 567–574.
[14] C. Claser, N.M. Espindola, G. Sasso, A.J. Vaz, S.B. Boscardin, M.M. Rodrigues, Immunologically relevant strain polymorphism in the Amastigote Surface Protein 2 of *Trypanosoma cruzi*, Microbes Infect. 9 (2007) 1011–1019.
[15] A.V. Machado, J.E. Cardoso, C. Claser, M.M. Rodrigues, R.T. Gazzinelli, O. Bruna-Romero, Long-term protective immunity induced against *Trypanosoma cruzi* infection after vaccination with recombinant adenoviruses encoding amastigote surface protein-2 and trans-sialidase, Hum. Gene Ther. 17 (2006) 898–908.
[16] H.J. Fehling, W. Swat, C. Laplace, R. Kuhn, K. Rajewsky, U. Muller, H. von Boehmer, MHC class I expression in mice lacking the proteasome subunit LMP-7, Science 265 (1994) 1234–1237.
[17] L. Van Kaer, P.G. Ashton-Rickardt, M. Eichelberger, M. Gaczynska, K. Nagashima, K.L. Rock, A.L. Goldberg, P.C. Doherty, S. Tonegawa, Altered peptidase and viral-specific T cell response in LMP2 mutant mice, Immunity 1 (1994) 533–541.
[18] S. Murata, H. Udono, N. Tanahashi, N. Hamada, K. Watanabe, K. Adachi, T. Yamano, K. Yui, N. Kobayashi, M. Kasahara, K. Tanaka, T. Chiba, Immunoproteasome assembly and antigen presentation in mice lacking both PA28alpha and PA28beta, Embo J. 20 (2001) 5898–5907.
[19] M. Rechsteiner, C. Realini, V. Ustrell, The proteasome activator 11 S REG (PA28) and class I antigen presentation, Biochem. J. 345 (Pt 1) (2000) 1–15.
[20] M. Groettrup, A. Soza, M. Eggers, L. Kuehn, T.P. Dick, H. Schild, H.G. Rammensee, U.H. Koszinowski, P.M. Kloetzel, A role for the proteasome regulator PA28alpha in antigen presentation, Nature 381 (1996) 166–168.
[21] P.M. Kloetzel, F. Ossendorp, Proteasome and peptidase function in MHC-class-I-mediated antigen presentation, Curr. Opin. Immunol. 16 (2004) 76–81.
[22] J. Driscoll, M.G. Brown, D. Finley, J.J. Monaco, MHC-linked LMP gene products specifically alter peptidase activities of the proteasome, Nature 365 (1993) 262–264.
[23] M. Gaczynska, K.L. Rock, A.L. Goldberg, Gamma-interferon and expression of MHC genes regulate peptide hydrolysis by proteasomes, Nature 365 (1993) 264–267.
[24] A.K. Vaidian, L.M. Weiss, H.B. Tanowitz, Chagas' disease and AIDS, Kinetoplastid Biol. Dis. 3 (2004) 2.